Disrupting Two *Arabidopsis thaliana* Xylosyltransferase Genes Results in Plants Deficient in Xyloglucan, a Major Primary Cell Wall Component [W][OA]

David M. Cavalier,[a] Olivier Lerouxel,[a,1] Lutz Neumetzler,[b] Kazuchika Yamauchi,[c] Antje Reinecke,[c] Glenn Freshour,[d] Olga A. Zabotina,[d,2] Michael G. Hahn,[e] Ingo Burgert,[c] Markus Pauly,[a,b] Natasha V. Raikhel,[d] and Kenneth Keegstra[a,f,g,3]

[a] Department of Energy Plant Research Laboratory, Michigan State University, East Lansing, Michigan 48824
[b] Max-Planck Institute for Molecular Plant Physiology, D-14476 Potsdam-Golm, Germany
[c] Department of Biomaterials, Max-Planck Institute of Colloids and Interfaces, D-14424 Potsdam-Golm, Germany
[d] Institute for Integrative Genome Biology, Center for Plant Cell Biology, Department of Botany and Plant Sciences, University of California, Riverside, California 92521
[e] Complex Carbohydrate Research Center, University of Georgia, Athens, Georgia 30602
[f] Department of Plant Biology, Michigan State University, East Lansing, Michigan 48824
[g] Department of Biochemistry and Molecular Biology, Michigan State University, East Lansing, Michigan 48824

Xyloglucans are the main hemicellulosic polysaccharides found in the primary cell walls of dicots and nongraminaceous monocots, where they are thought to interact with cellulose to form a three-dimensional network that functions as the principal load-bearing structure of the primary cell wall. To determine whether two *Arabidopsis thaliana* genes that encode xylosyltransferases, *XXT1* and *XXT2*, are involved in xyloglucan biosynthesis in vivo and to determine how the plant cell wall is affected by the lack of expression of *XXT1*, *XXT2*, or both, we isolated and characterized *xxt1* and *xxt2* single and *xxt1 xxt2* double T-DNA insertion mutants. Although the *xxt1* and *xxt2* mutants did not have a gross morphological phenotype, they did have a slight decrease in xyloglucan content and showed slightly altered distribution patterns for xyloglucan epitopes. More interestingly, the *xxt1 xxt2* double mutant had aberrant root hairs and lacked detectable xyloglucan. The reduction of xyloglucan in the *xxt2* mutant and the lack of detectable xyloglucan in the *xxt1 xxt2* double mutant resulted in significant changes in the mechanical properties of these plants. We conclude that *XXT1* and *XXT2* encode xylosyltransferases that are required for xyloglucan biosynthesis. Moreover, the lack of detectable xyloglucan in the *xxt1 xxt2* double mutant challenges conventional models of the plant primary cell wall.

INTRODUCTION

Growing plant cells are surrounded by a primary cell wall that provides mechanical support yet is sufficiently dynamic to allow cells to expand. In some cells, secondary cell walls are constructed between the primary cell wall and the plasma membrane after expansion has ceased, and they often contribute to specialized functions related to a specific cell type, such as xylem fibers, tracheids, and sclereids. The plant cell wall is a complex structure that is composed of cellulose, hemicellulose, pectin, protein, lignin, and various inorganic compounds (Carpita and McCann, 2000). The hemicelluloses are complex polysaccharides that are thought to play an important role in the structure and function of primary and secondary cell walls and include xyloglucan (XyG), xylans, mannans, and mixed-linkage glucans (O'Neill and York, 2003; Obel et al., 2007). The cell walls of all vascular plants analyzed thus far, including lycopodiophytes (extant primitive vascular plants), gymnosperms, and angiosperms, have been found to contain XyG (O'Neill and York, 2003; Popper and Fry, 2004; Hoffman et al., 2005). In the primary cell walls of graminaceous monocots, where xylans and mixed-linkage glucans are the major hemicelluloses, XyG comprises only 1 to 5% of the cell wall dry weight (Carpita and Gibeaut, 1993; O'Neill and York, 2003). By contrast, XyG is the major hemicellulose found in the primary cell walls of dicots and nongraminaceous monocots, where it constitutes 10 to 20% of the cell wall dry weight (Fry, 1989; Hayashi, 1989; O'Neill and York, 2003).

XyG is composed of a β-(1→4)-glucan backbone that is substituted with α-(1→6)-xylosyl residues in a regular pattern. Although there is variation in the xylose substitution patterns among different plant species (Hoffman et al., 2005), most species of plants have either XXXG-type or XXGG-type XyG (Vincken et al., 1997) (see Figure 3 legend for a description of XyG

---

nomenclature). Specific xylosyl residues, and in some cases specific glucosyl residues of the glucan backbone, are further substituted with a variety of glycosyl residues or disaccharides (see Figure 1 in Obel et al. [2007]). For example, *Arabidopsis thaliana* XyG is composed of XXXG repeating subunits that can be further substituted at the O-2 position of specific Xyl residues with either a β-D-Gal*p* or a disaccharide composed of α-L-Fuc*p*-(1→2)-β-D-Gal*p*. Thus, *Arabidopsis* XyG hydrolyzed with endoglucanase will release predominately XXXG, XXFG, and XLFG and minor amounts of XXLG, XLLG, and XLXG (Lerouxel et al., 2002; Vanzin et al., 2002; Madson et al., 2003). Finally, XyG can be *O*-acetylated at specific glycosyl residues that can vary between species (York et al., 1988, 1996; Kiefer et al., 1990; Maruyama et al., 1996; Lerouxel et al., 2002); however, the biological purpose and mechanism of XyG acetylation is unknown (Obel et al., 2007).

Much is known about the structure and prevalence of XyG, yet the function of XyG in the primary cell wall remains poorly understood. Because many studies have shown that XyG forms strong noncovalent interactions with cellulose (for reviews, see Fry [1989], Hayashi [1989], Carpita and Gibeaut [1993], and Obel et al. [2007]), XyG is featured prominently in many models of the primary cell wall. Most models predict that XyG functions as a tether by cross-linking adjacent cellulose microfibrils, thereby forming a cellulose-XyG network that functions as the primary load-bearing structure of the primary cell wall during cell expansion (Fry and Miller, 1989; Hayashi, 1989; McCann and Roberts, 1991; Passioura and Fry, 1992; Carpita and Gibeaut, 1993; Veytsman and Cosgrove, 1998; Somerville et al., 2004). Other models predict that XyG acts either as a spacer to prevent the cellulose microfibrils from aggregating (Thompson, 2005) or as an adapter that enables cellulose to interface with other cell wall matrix components (Keegstra et al., 1973; Talbott and Ray, 1992; Ha et al., 1997). Although XyG plays a prominent role in most models of the primary cell wall, the function of XyG in the structure and growth of the primary cell wall remains to be demonstrated conclusively.

Because XyG has been predicted to play a central role in the primary cell wall during growth, identification and characterization of the genes that encode XyG biosynthetic enzymes are important research areas. Predictably, the biosynthesis of XyG requires the activities of a β-glucan synthase; at least one, and possibly several, α-xylosyltransferases (XTs); at least two β-galactosyltransferases; an α-fucosyltransferase (Lerouxel et al., 2006); as well as additional enzymes, such as nucleotide sugar transporters and nucleotide sugar interconversion enzymes (Seifert et al., 2004; Nguema-Ona et al., 2006; Obel et al., 2007).

Recently, Cocuron et al. (2007) used transcription profiling of developing nasturtium (*Tropaeolum majus*) seeds, in which XyG is the primary seed storage polysaccharide, to identify a gene that has high sequence similarity to an *Arabidopsis cellulose synthase-like* (*CSL*) gene, *CSLC4*, which belongs to CAZy family GT2 (Campbell et al., 1997; Coutinho et al., 2003). Cocuron et al. (2007) showed that both *CSLC* from *T. majus* and *CSLC4* from *Arabidopsis* encode proteins with β-glucan synthase activity when expressed in the methylotrophic yeast *Pichia pastoris*. The experimental evidence produced by Cocuron et al. (2007) along with other arguments that they presented provided compelling evidence that this β-glucan synthase activity is involved in XyG biosynthesis.

Progress has been made in identifying the genes that encode the XyG glycosyltransferases involved in the addition of the various XyG side chains to the β-glucan backbone. Perrin et al. (1999) used traditional biochemical techniques to purify XyG fucosyltransferase activity from pea (*Pisum sativum*) seedlings. Using the amino acid sequence information derived from the purified protein, genes encoding XyG fucosyltransferases from *Arabidopsis* (At *FUT1*) (Perrin et al., 1999) and pea (Ps *FUT1*) (Faik et al., 2000) were identified. Subsequently, the reduction in fucose content observed in crude cell wall preparations of the *murus2* (*mur2*) mutant (Reiter et al., 1997) was shown to be due to a lesion in At *FUT1*, which caused a 99% reduction in fucosylated XyG (Vanzin et al., 2002). Furthermore, heterologous expression and genetic studies indicate that At *FUT1*, which is part of the multigene family of fucosyltransferases (Sarria et al., 2001) that belong to CAZy family GT34, is the only fucosyltransferase gene required for XyG biosynthesis (Vanzin et al., 2002; Perrin et al., 2003).

Madson et al. (2003) showed that the reduction in fucose content of the *mur3-1* and *mur3-2* mutants (Reiter et al., 1997) was due to lesions in a XyG galactosyltransferase gene. XyG derived from mutant plants lacked significant amounts of XXLG, XXFG, and XLFG subunits and had significant increases in the proportion of XXXG and XLXG subunits (Lerouxel et al., 2002; Madson et al., 2003). Moreover, when incubated with *mur3*-derived XyG, *Pichia*-expressed *MUR3* only galactosylated the first xylosyl residue from the reducing end of the XXXG repeating subunit to produce XXLG (Madson et al., 2003). Results from this study indicate that in addition to *MUR3*, which is a member of a large *Arabidopsis* gene family that belongs to CAZy family GT47, at least one other galactosyltransferase is required for XyG biosynthesis (Madson et al., 2003; Li et al., 2004).

Faik et al. (2002) identified a seven-member family of candidate *Arabidopsis* XyG XT (XXT) genes that belong to CAZy family GT34. This family also contains the fenugreek galactomannan galactosyltransferase identified by Edwards et al. (1999). To investigate the hypothesis that some or all of the *Arabidopsis* genes in this family encode XXTs, they were expressed in heterologous systems, and the activity of the resulting proteins was examined. Results from these analyses showed that the closely related *XXT1* and *XXT2* (formerly At *XT1* and At *XT2*, respectively) encode enzymes with XT activities that are capable of transferring Xyl from UDP-Xyl to an array of acceptor substrates to form nascent XyG oligosaccharides (Faik et al., 2002; Cavalier and Keegstra, 2006; Fauré et al., 2007). Furthermore, when cellohexaose was used as an acceptor substrate, XXT1 and XXT2 exhibited the same preferences for the location of xylose addition and were capable of catalyzing the addition of multiple xylosyl residues (Cavalier and Keegstra, 2006).

To address whether XXT1 or XXT2 is involved in XyG biosynthesis in vivo and to determine how the plant cell wall was affected by mutations in *XXT1*, *XXT2*, or both, we isolated and characterized *xxt1* and *xxt2* single and *xxt1 xxt2* double T-DNA insertion lines. In this report, we present results from our characterization of these mutants. Whereas the *xxt1* and *xxt2* single mutants had a modest reduction in XyG content, the most surprising finding of this study was that the *xxt1 xxt2* double mutant lacked detectable XyG. From these results we conclude that *XXT1* and *XXT2* encode XTs that are involved in XyG biosynthesis in vivo. Yet, given the

importance of the cellulose-XyG network in many models of the primary cell wall, the lack of detectable XyG in the *xxt1 xxt2* double mutant plants challenges conventional models for the functional organization of components in primary cell walls.

RESULTS

xxt1 xxt2 Double Mutants Display a Severe Root Hair Phenotype

The ability of XXT1 and XXT2 to synthesize XyG-like oligosaccharides when expressed in heterologous systems (Faik et al., 2002; Cavalier and Keegstra, 2006) led us to predict that disruption of the synthesis of these enzymes in planta would have a measurable impact not only on XyG structure but also on the organization of the primary cell wall. To test this prediction, we isolated and characterized homozygous *xxt1* and *xxt2* T-DNA insertion lines from the Syngenta and Salk collections, respectively (Figure 1A). RT-PCR analysis confirmed that T-DNA insertion lines lacked transcripts derived from their respective genes (Figure 1B). Yet, these mutants were, for the most part, morphologically indistinguishable from the wild type, which led us to hypothesize that *XXT1* and *XXT2* are genetically redundant. To test for genetic redundancy, we crossed the *xxt1* and *xxt2* single mutants and used PCR screening to identify *xxt1 xxt2* double mutants in the resulting F2 generation. We identified two double mutants out of a total of 218 F2 plants, which is significantly lower

($\chi^2 = 10.58$; $P < 0.01$) than the $\sim$14 plants that were expected from a Mendelian ratio of 1:16. Although we do not understand why the F2 double mutants were recovered at such a low frequency, we did not encounter any problems with the subsequent propagation of the homozygous *xxt1 xxt2* double mutants.

Analysis of the double mutant plants using RT-PCR verified the lack of both *XXT1* and *XXT2* transcripts (Figure 1B). Compared with wild-type, *xxt1*, or *xxt2* plants, the *xxt1 xxt2* double mutant plants grew more slowly, were smaller at maturity (see Supplemental Figures 1A and 1B online), and had a severe root hair phenotype (Figures 2A to 2H). In contrast with either wild-type (Figures 2A, 2E, and 2G) or single mutant plants (Figures 2B and 2C), *xxt1 xxt2* seedlings (Figures 2D, 2F, and 2H) had short root hairs with bulging bases. The normal root hair phenotype was restored when the *xxt1 xxt2* double mutant was complemented with either *35S_{pro}:XXT1* or *35S_{pro}:XXT2* (Figures 2I and 2J).

Given that plant cell wall models predict that XyG is a major structural component of the primary cell wall, we hypothesized that the deformed root hairs of the *xxt1 xxt2* double mutant were a result of aberrant XyG biosynthesis that caused the cell walls to be weaker in these specialized cells. To test this hypothesis, we sought to determine whether the mutants had either altered levels of XyG or modified XyG structure in tissues throughout the plants.

xxt1 xxt2 Seedlings Lack XEG-Susceptible XyG

Oligosaccharide mass profiling (OLIMP) is a method that employs the sensitivity of matrix-assisted laser desorption ionization
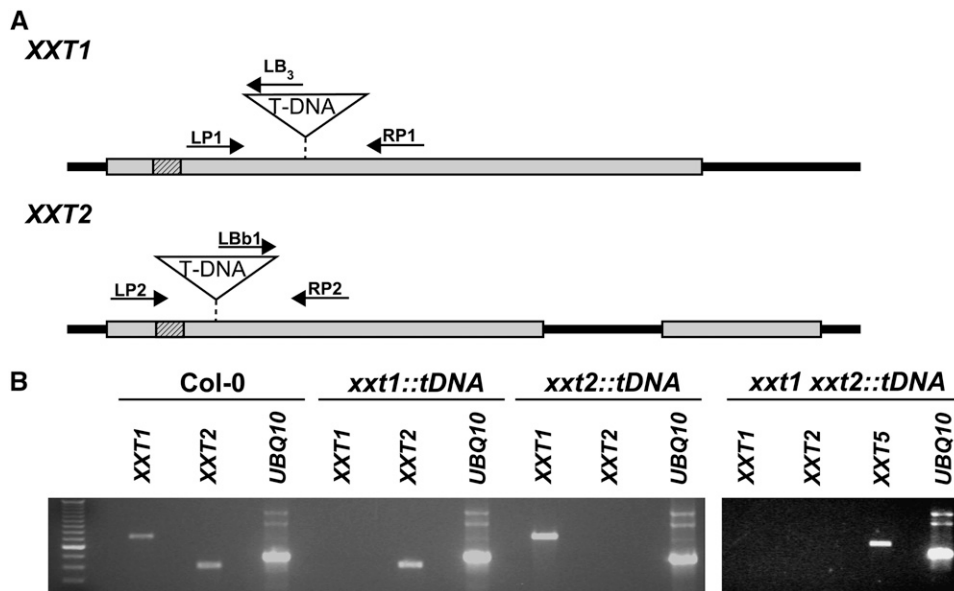

Figure 1. Analysis of *xxt1*, *xxt2*, and *xxt1 xxt2* T-DNA Insertion Mutants.

(A) Gene models of *XXT1* and *XXT2*. Noncoding regions and introns are represented by heavy black lines; coding regions are represented by gray rectangles. The black box with diagonal lines represents the predicted transmembrane domain encoded by each gene. The T-DNA insertion site for each gene is indicated. The position and orientation of each primer is also indicated.

(B) RT-PCR analysis of wild-type (Columbia [Col-0]) and T-DNA insertion mutants. Total RNA was isolated from 7-d-old wild-type, *xxt1*, *xxt2*, and *xxt1 xxt2* mutant seedlings and digested twice with DNase. Wild-type and T-DNA insertion lines were assayed for the presence of *XXT1* and *XXT2* transcripts with RT-PCR for 35 cycles with gene-specific primers (see Supplemental Table 2 online). The experiment was conducted on three different pools of 7-d-old etiolated seedlings from each line, and the typical result of an ethidium bromide–stained agarose gel is presented.
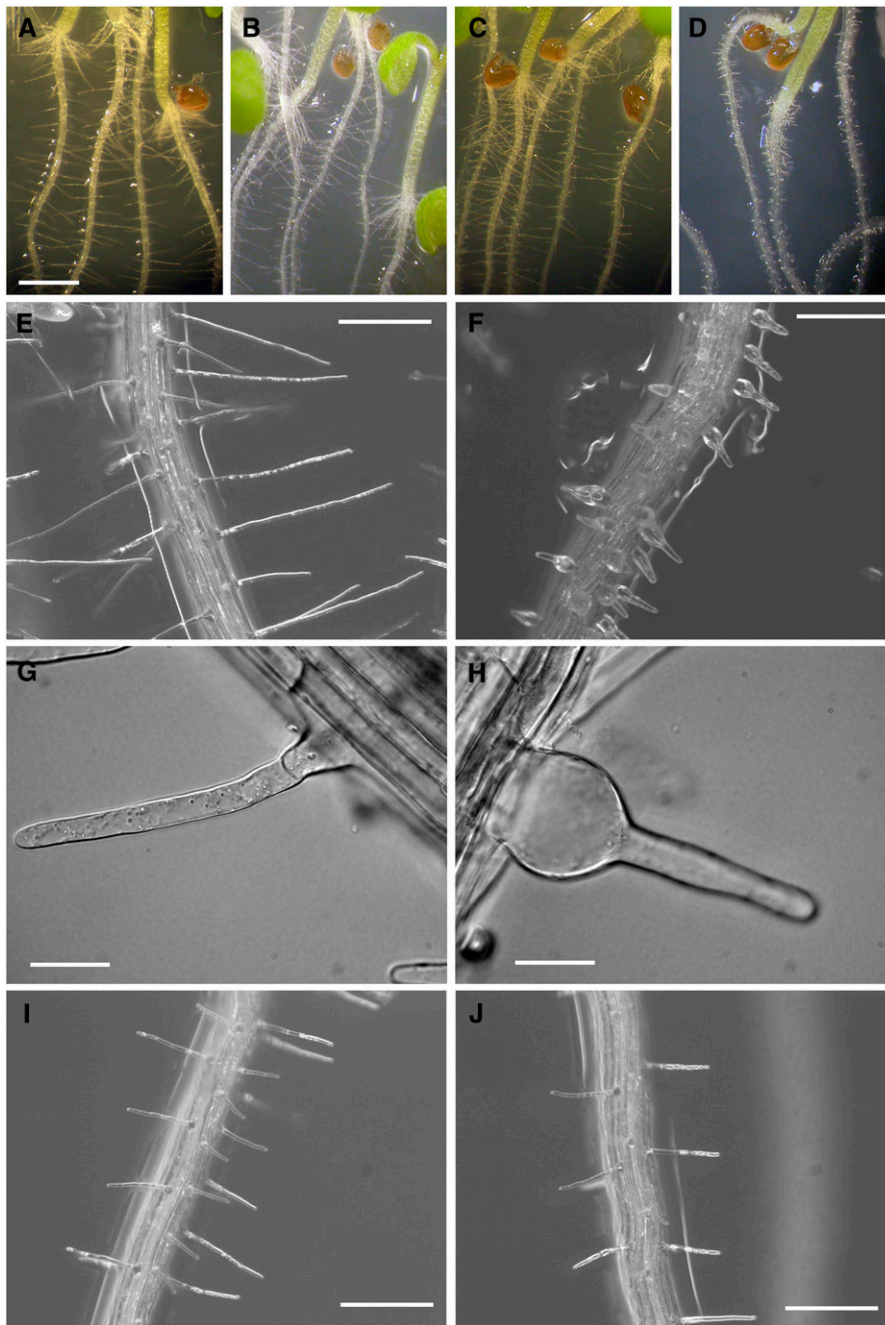
Figure 2. The *xxt1 xxt2* T-DNA Insertion Mutant Has a Root Hair Phenotype.

(A) to **(D)** Seven-day-old seedlings of wild-type, *xxt1*, *xxt2*, and *xxt1 xxt2* grown on vertical agar plates. Bar = 1 mm.
(E) Wild-type root hairs. Bar = 200 μm.
(F) *xxt1 xxt2* root hairs. Bar = 200 μm.
(G) Representative example of a wild-type root hair located just above the zone of elongation. Bar = 50 μm.
(H) Representative example of an *xxt1 xxt2* double mutant root hair located just above the zone of elongation. Bar = 25 μm.
(I) and **(J)** Root hairs of *xxt1 xxt2* double mutants (T2 generation) complemented with either $35S_{pro}:XXT1$ **(I)** or $35S_{pro}:XXT2$ **(J)**. Bars = 200 μm.

time-of-flight mass spectrometry (MALDI-TOF-MS) and the specificity of XyG-specific *endo*-β-1,4-glucanase (XEG) to rapidly determine the relative abundance of XyG oligosaccharides released from a variety of cell wall preparations (Pauly et al., 1999b; Lerouxel et al., 2002). We chose to use crude cell wall preparations (alcohol-insoluble residue [AIR]) for OLIMP and other biochemical analyses to minimize the possibility of losing cell wall polysaccharides, which may occur when a more exhaustive cell wall isolation protocol is used.

Results of the OLIMP analysis demonstrated that there was no significant difference in the relative abundance of XyG oligosaccharides released from AIR preparations derived from 4-d-old etiolated seedlings of wild-type and *xxt1* or *xxt2* plants (Figure 3A).

However, XEG-digested AIR from the *xxt1 xxt2* double mutant did not produce any characteristic XyG oligosaccharide-specific ions. To confirm this result, high-performance anion-exchange chromatography-pulsed amperometric detection (HPAEC-PAD) analysis was performed on XEG digestions of AIR derived from *xxt1 xxt2* and wild-type seedlings. Control samples from wild-type plants showed the expected XyG oligosaccharides (Figure 3B), whereas samples from the double mutant plants lacked XyG oligosaccharides (Figure 3C).

Results of OLIMP analysis indicated that the *xxt1 xxt2* double mutant did not have detectable XyG. However, there are two issues to consider when interpreting these results: XEG substrate accessibility and substrate specificity. Pauly et al. (1999a)
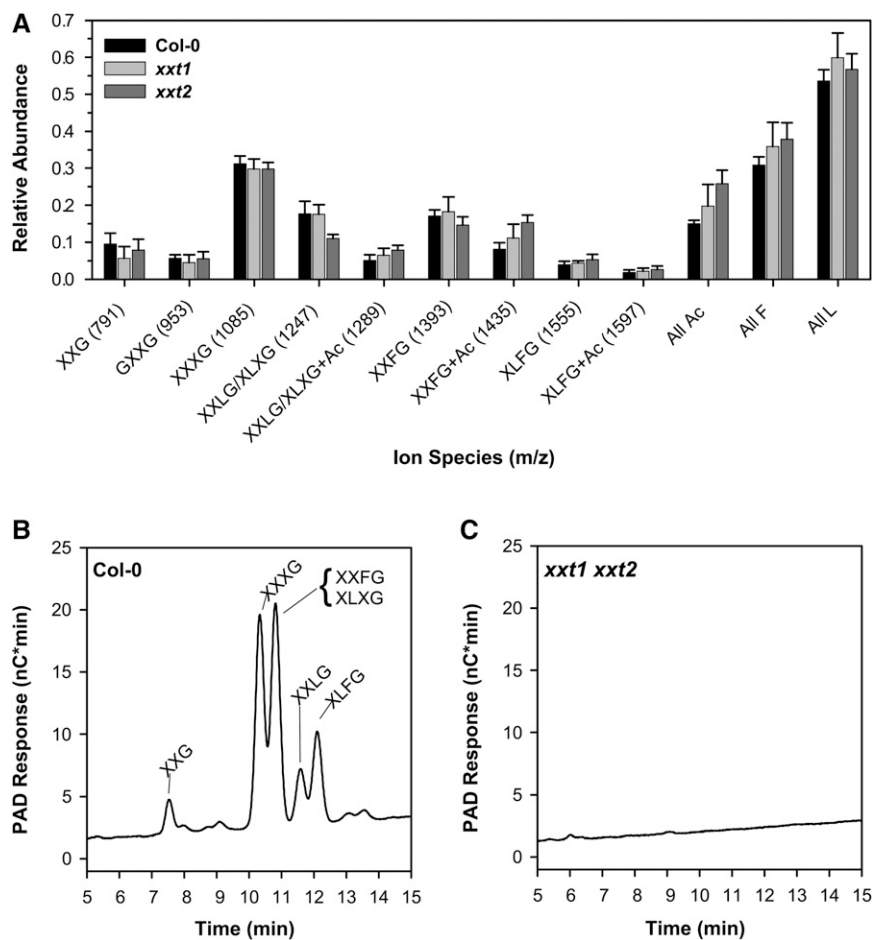

Figure 3. OLIMP of XyG Oligosaccharides Released by XyG-Specific Endoglucanase.

(A) OLIMP of XyG oligosaccharides released from AIR preparations of 4-d-old wild-type (Col-0), *xxt1*, and *xxt2* etiolated seedlings digested with XEG. The relative abundance of XyG oligosaccharide is presented as mean value ($n = 6$ hypocotyls) ± SD. The *m/z* of each XyG oligosaccharide is presented in parentheses. All Ac, total relative amount of acetylated XyG oligosaccharides; All F, total relative amount of fucosylated XyG oligosaccharides; All L, total relative amount of galactosylated XyG oligosaccharides.

(B) and **(C)** HPAEC chromatograms of a crude cell wall preparation of 7-d-old wild-type **(B)** and *xxt1 xxt2* double mutant **(C)** etiolated seedlings digested with XEG. Each XyG oligosaccharide is named according to a XyG nomenclature detailed by Fry et al. (1993), where the XyG molecule is described from the nonreducing end to the reducing end with a single letter that denotes a specific glucosyl residue substitution pattern. An unsubstituted β-glucan backbone D-Glc*p* is assigned "G," an α-D-Xyl*p*-(1→6)-β-D-Glc*p* substitution pattern is assigned "X," a β-D-Gal*p*-(1→2)-α-D-Xyl*p*-(1→6)-β-D-Glc*p* substitution pattern is assigned "L," and an α-L-Fuc*p*-(1→2)-β-D-Gal*p*-(1→2)-α-D-Xyl*p*-(1→6)-β-D-Glc*p* substitution pattern is assigned "F." PAD, pulsed amperometric detector.

described the macromolecular organization of the cellulose-XyG network of higher plants based on the sequential extraction of XyG with XEG, KOH, and cellulase. The XEG-susceptible fraction composes ~38% of the total XyG and is thought to represent a domain of XyG that spans adjacent cellulose microfibrils. Therefore, OLIMP analysis provides a measure of the amount of XyG in this domain and only if XEG has access to this domain. As to XEG substrate specificity, XEG has been shown to use only XyG as a substrate Pauly et al. (1999b), so it is possible that the *xxt1 xxt2* double mutant has structurally aberrant XyG that is not recognized by XEG. To gain further insight into these possibilities and to gain an understanding of the cell-specific distribution of wall components in these mutants, we performed immunohistochemical studies with a suite of monoclonal antibodies directed against cell wall polysaccharides.

Immunohistochemistry of Wild-Type, *xxt1*, *xxt2*, and *xxt1 xxt2* Mutants

The structural defects of *xxt1 xxt2* double mutant root hairs led us to probe root sections of 7-d-old seedlings with monoclonal antibodies directed against cell wall polysaccharides, including XyG (CCRC-M1, CCRC-M39, CCRC-M58, CCRC-M87, and CCRC-M89), homogalacturonan (CCRC-M34, CCRC-M38, JIM5, and JIM7), rhamnogalacturonan I (RG-I; CCRC-M2), arabinogalactan (JIM13 and JIM19), and xylan (LM10 and LM11).

There were significant differences in the labeling patterns and intensities in the mutant lines for antibodies that recognize XyG: CCRC-M1, CCRC-M39, CCRC-M58, CCRC-M87, and CCRC-M89 (Figure 4). Each XyG-directed antibody shows a distinct labeling pattern in wild-type roots (Figures 4A to 4E), with CCRC-M1, CCRC-M39, and CCRC-M87 labeling most walls in the sections, albeit with varying intensities and uniformity, while CCRC-M58 and CCRC-M89 label primarily the root hair walls and, to a lesser extent, phloem.

The labeling patterns observed in the roots of the *xxt1* and *xxt2* single mutants were different from wild-type plants, though in distinct ways (Figures 4F to 4O). In the *xxt1* single mutant, the labeling patterns of CCRC-M1, CCRC-M39, and CCRC-M87 were very similar to the labeling patterns found in wild-type roots. However, CCRC-M58 and CCRC-M89 showed increased labeling of walls in cell types (e.g., cortex and endodermis) with respect to wild-type roots. Labeling of the *xxt2* single mutant with CCRC-M39 and CCRC-M87 was reduced and was less uniform across all cell types in comparison with wild-type roots. CCRC-M58 and CCRC-M89 show increased labeling of walls in the body of root hair–forming cells, which has not been observed in wild-type roots. We interpreted these results as evidence that XyG content or XyG structure was slightly perturbed in the *xxt1* and *xxt2* single mutants.

Most significant was the absence of labeling with XyG-directed antibodies in the *xxt1 xxt2* double mutant (Figures 4P to 4T). In addition to the five antibodies shown in Figure 4, 17 other XyG-directed antibodies (see Supplemental Table 1 online) were tested on root sections of the *xxt1 xxt2* double mutant, and none of them showed any immunofluorescent labeling. This group of antibodies included those against XyG epitopes not detected in wild-type *Arabidopsis* plants. Thus, the absence of labeling is

evidence that the double mutant did not synthesize any altered XyG containing structures recognized by these antibodies.

Antibodies directed against epitopes commonly found in other non-XyG polysaccharides in plant cell walls were used to test if the mutations in *XXT1*, *XXT2*, or both affected other wall components. No significant differences between wild-type and the mutant lines were detected in either label intensity or labeling patterns of the non-XyG antibodies used (see Supplemental Figure 2 online). In particular, the distribution of the xylan epitopes recognized by LM10 and LM11 was unaffected by the mutations (see Supplemental Figures 2GG and 2HH online), which is evidence against compensatory upregulation of xylan biosynthesis. Some subtle differences in the distribution patterns and intensities of several pectin-directed antibodies were noted in *xxt2*, namely, CCRC-M2, JIM5, and CRCC-M34 (see Supplemental Figures 2S, 2U, and 2V online). The fact that non-XyG-directed antibodies labeled the *xxt1 xxt2* double mutant is evidence that the absence of labeling using XyG-directed antibodies was unlikely to have been caused by a reduction in epitope access.

Consistent with the results from OLIMP analysis of crude cell wall preparations, immunohistochemical analysis showed that the *xxt1 xxt2* double mutant lacked detectable XyG. However, similar to the aforementioned substrate specificity caveat for XEG, the XyG-directed antibodies may recognize only a limited set of XyG epitopes. Thus, it is still possible that the *xxt1 xxt2* double mutant had XyG that is structurally distinct and was not recognized by these antibodies. Therefore, to further investigate the immunohistochemical and OLIMP results, we performed more detailed biochemical analyses.

Glycosyl Residue Composition Analysis of AIR Preparations

Glycosyl residue composition analysis was performed to determine whether there was a significant difference in the monosaccharide content of crude cell wall preparations between the wild type and the mutants. Seven-day-old etiolated seedlings were chosen to minimize the effects of glucose from starch in glycosyl residue composition and glycosyl linkage analyses (see below). Glycosyl residue composition analysis was done by sequential treatment of AIR preparations with trifluoroacetic acid (TFA) hydrolysis, followed by Saeman hydrolysis of TFA hydrolysis-resistant material. Treatment of cell wall material by TFA hydrolysis liberates monosaccharides from noncellulosic polysaccharides and amorphous cellulose (Fry, 2000); Saeman hydrolysis releases sugars from crystalline cellulose and any remaining noncellulosic polysaccharides (Selvendran et al., 1979).

Analysis of the monosaccharides liberated from crude cell walls of 7-d-old etiolated seedlings by TFA hydrolysis (Table 1) showed that there were no differences between wild-type and mutant lines in the amounts of mannose, glucose, or uronic acids (galacturonic and glucuronic acids). However, significant decreases (unless noted, $P < 0.025$ was considered statistically significant in all experiments) in rhamnose, fucose, arabinose, xylose, and galactose were observed in all three mutant lines when the results were expressed as amounts of sugar per mass of crude cell wall material. Furthermore, the *xxt1 xxt2* double mutant had significantly lower levels of fucose, xylose, and galactose than either the *xxt1* or *xxt2* single mutants. When the same
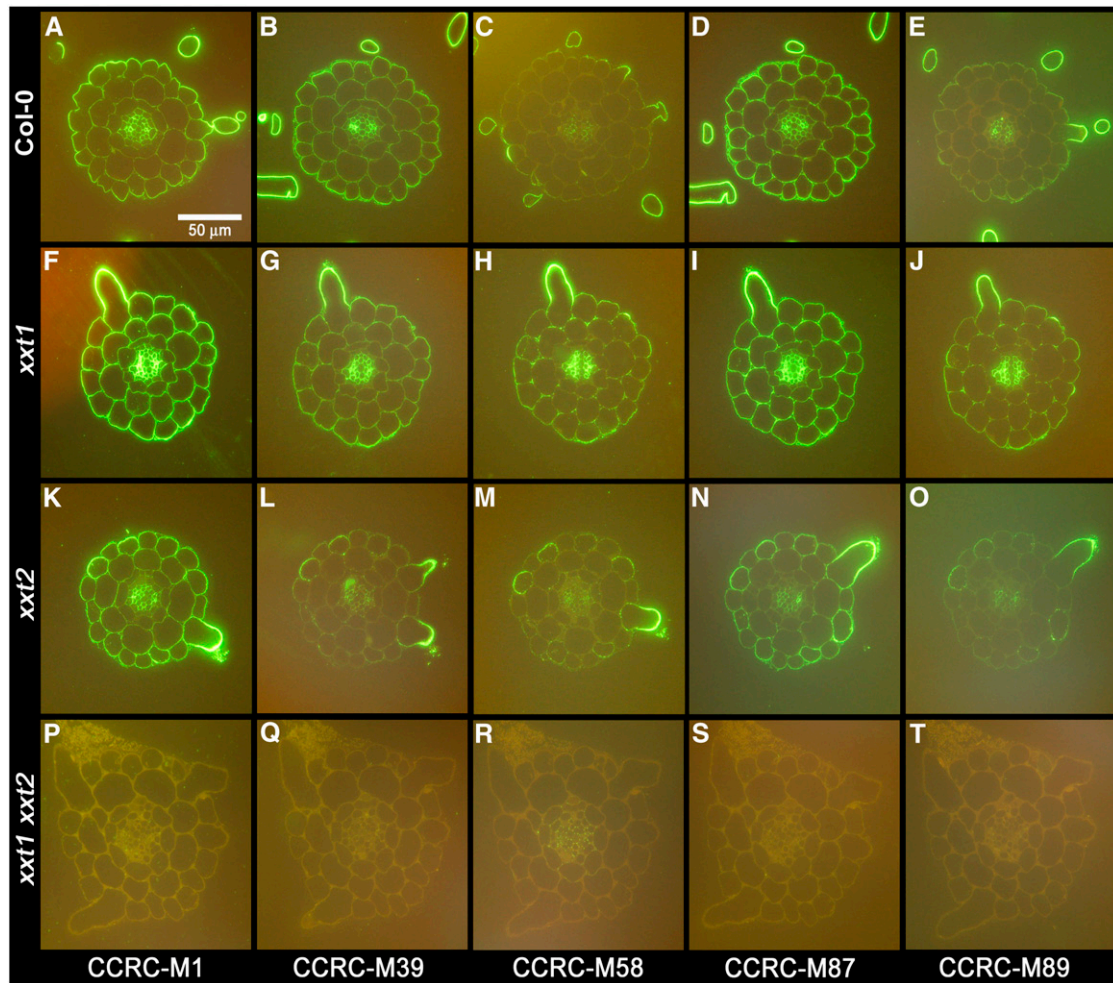
Figure 4. Immunofluorescent Labeling of Wild-Type and Mutant Roots with XyG-Directed Antibodies.

Immunofluorescent labeling of 250-nm transverse sections taken from ∼5 mm above the root apex of 4-d-old wild-type (Col-0), *xxt1*, *xxt2*, and *xxt1 xxt2* seedlings. The antibodies used were directed against different epitopes of XyG and are described in Methods.
(A) to **(E)** Col-0 root cross-sections labeled with CCRC-M1 **(A)**, CCRC-M39 **(B)**, CCRC-M58 **(C)**, CCRC-M87 **(D)**, and CCRC-M89 **(E)**.
(F) to **(J)** *xxt1* single mutant root cross-sections labeled with CCRC-M1 **(F)**, CCRC-M39 **(G)**, CCRC-M58 **(H)**, CCRC-M87 **(I)**, and CCRC-M89 **(J)**.
(K) to **(O)** *xxt2* single mutant root cross-sections labeled with CCRC-M1 **(K)**, CCRC-M39 **(L)**, CCRC-M58 **(M)**, CCRC-M87 **(N)**, and CCRC-M89 **(O)**.
(P) to **(T)** *xxt1 xxt2* double mutant root cross-sections labeled with CCRC-M1 **(P)**, CCRC-M39 **(Q)**, CCRC-M58 **(R)**, CCRC-M87 **(S)**, and CCRC-M89 **(T)**.

data are expressed in terms of mole percent of the recovered sugars rather than micrograms of monosaccharides per milligram of crude cell wall, no differences were noted in the distribution of the relative amount of each monosaccharide in either *xxt1* or *xxt2* mutant lines, with respect to the wild type (see Supplemental Figure 3 online). However, there were decreases in the mole percents of fucose, xylose, and galactose in the *xxt1 xxt2* double mutant, with respect to the wild type. The reductions in fucose, galactose, and xylose, whether in terms of either micrograms of monosaccharide per milligram AIR or mole percent, would be expected if the XTs involved in XyG biosynthesis were disrupted.

Composition analysis of Saeman-hydrolyzed TFA-resistant material (Table 1) showed the presence of glucose (>96% of the total monosaccharides present) and trace amounts of other monosaccharides, which indicated that TFA hydrolysis was

virtually complete. Although the *xxt1* and *xxt2* mutants did not have significantly less glucose than the wild type in the TFA-resistant pellet, there was a significant decrease (P values of 0.048 and 0.251 for the *xxt1* and *xxt2* mutants, respectively) in the amount of glucose in the TFA-resistant material of the *xxt1 xxt2* double mutant, which led us to conclude that this mutant has less cellulose than the wild-type plants.

Glycosyl Linkage Analysis

If *XXT1* and *XXT2* encode XTs involved in XyG biosynthesis, we would expect glycosyl residues associated with XyG to be affected by disruption of these genes; therefore, we performed linkage analysis via methylation of the polysaccharides followed by hydrolysis and analysis of the resulting partially methylated

Table 1. Monosaccharide Composition Analysis of AIRs from 7-d-Old Etiolated Seedlings

Treatment	Monosaccharides (µg mg^{-1} AIRs)								
	Rhamnose[a]	Fucose[a]	Arabinose[a]	Xylose[a]	Mannose[a,b]	Galactose[a]	Glucose[a]	Galacturonic Acid[c]	Glucuronic Acid[c]
TFA hydrolysis									
Col-0	26.40 ± 1.79	2.24 ± 0.14	19.96 ± 1.14	19.46 ± 1.22	7.80 ± 0.48	28.71 ± 1.73	32.77 ± 3.01	31.68 ± 4.81	3.78 ± 0.75
xxt1	19.73 ± 1.41*	1.36 ± 0.23*	15.89 ± 1.02*	13.63 ± 0.84*	6.30 ± 0.33	21.05 ± 1.16*	27.82 ± 1.51	28.42 ± 4.01	3.00 ± 0.23
xxt2	20.77 ± 0.91*	1.29 ± 0.05*	16.03 ± 0.67*	13.96 ± 0.72*	7.15 ± 0.37	22.33 ± 1.20*	26.22 ± 1.13	30.70 ± 0.31	3.42 ± 0.01
xxt1 xxt2	20.17 ± 2.02*	0.48 ± 0.07*	16.59 ± 1.44*	9.88 ± 1.53*	6.98 ± 0.08	16.53 ± 1.43*	29.56 ± 3.42	29.25 ± 1.71	2.41 ± 0.21
Saeman hydrolysis									
Col-0	0.23 ± 0.02	ND	0.28 ± 0.09	1.06 ± 0.09	2.72 ± 0.15	0.39 ± 0.10	137.89 ± 9.96	–	–
xxt1	0.07 ± 0.04	ND	0.18 ± 0.05	0.90 ± 0.26	1.89 ± 0.15	0.21 ± 0.02	117.01 ± 7.25	–	–
xxt2	0.18 ± 0.08	ND	0.25 ± 0.10	0.92 ± 0.21	2.50 ± 0.41	0.29 ± 0.12	127.65 ± 8.62	–	–
xxt1 xxt2	0.08 ± 0.03	ND	0.11 ± 0.06	0.94 ± 0.33	2.03 ± 0.48	0.15 ± 0.04	106.50 ± 5.32*	–	–

[a] As determined by GC-MS analysis of alditol acetate derivatives of AIRs.
[b] The presence of mannose after Saeman hydrolysis probably represents glucose that has epimerized at the C-2 carbon (Carpita and Shea, 1989).
[c] As determined by HPAEC.
Values are derived from $n = 3$ biological replications ± SD. * Statistically significant difference with respect to the wild type (Col-0; $P < 0.025$). ND, not detected; –, not determined.

alditol acetates (PMAAs). Because we had significant problems with undermethylation of polysaccharides when crude cell wall preparations were analyzed, we fractionated the crude cell wall preparations into pectic and hemicellulosic fractions by hot ammonium oxalate and 4 N KOH, respectively, prior to methyl-ation. Results show that there were few differences in glycosyl linkages found in the ammonium oxalate fraction of the mutants with respect to the wild type (Table 2). However, in the 4 N KOH extract of the *xxt1 xxt2* double mutant, there was a reduction in peak areas of glycosyl residues that can be assigned to XyG,

Table 2. Glycosyl Residue Linkage Analysis of Fractionated Cell Walls of 7-d-Old Etiolated Seedlings

Fractions Residue[a]	Hot Ammonium Oxalate Extraction				4 N KOH Extraction			
	Col-0	xxt1	xxt2	xxt1 xxt2	Col-0	xxt1	xxt2	xxt1 xxt2
T-Fucp	1.7	1.9	1.6	1.8	0.9	1.3	1.0	0.5
2-Rhap	5.3	5.4	5.5	13.6	ND	ND	ND	ND
2,4-Rhap	4.0	4.6	4.6	1.0	ND	ND	ND	ND
T-Araf	7.6	6.0	6.5	8.9	2.3	3.2	3.5	5.0
2-Arap	ND	ND	ND	ND	1.8	3.0	4.3	1.9
3-Araf	7.5	4.8	5.0	5.6	1.8	1.4	1.7	0.0
5-Araf	18.8	11.0	14.4	17.7	3.4	3.2	3.9	6.6
T-Xylp	1.9	2.0	1.9	1.7	2.0	2.7	2.0	1.3
2-Xylp[b]	1.0	1.3	1.2	0.6	1.8	2.1	1.8	1.5
4-Xylp[b]	5.3	8.5	6.5	7.6	9.0	13.5	13.0	30.2
2,4-Xylp	4.3	4.0	6.3	3.4	2.3	3.3	3.8	2.9
T-Galp	7.3	9.7	10.0	12.9	1.8	2.2	2.0	3.8
2-Galp	ND	ND	ND	ND	3.3	3.6	2.9	1.9
4-Galp	8.5	6.9	6.9	10.0	3.7	1.8	1.8	2.4
T-Manp	ND	ND	ND	ND	1.1	1.6	2.4	4.2
4-Manp	ND	ND	ND	ND	3.8	4.2	4.7	8.1
4,6-Manp	ND	ND	ND	ND	4.7	2.7	2.8	5.1
T-Glcp	2.8	3.1	3.1	2.6	1.0	0.1	1.6	3.1
3-Glcp	ND	ND	ND	ND	5.2	5.6	7.8	5.4
4-Glcp	10.1	13.3	11.2	4.3	19.3	13.7	13.1	12.6
6-Glcp	4.5	4.0	3.8	4.2	1.6	1.2	1.8	1.3
4,6-Glcp	9.6	13.2	11.4	4.0	29.1	29.5	24.1	2.2

[a] Glycosyl residues are expressed as percentage of total peak areas.
[b] The peak area values for 2-Xyl and 4-Xyl were calculated by multiplying the relative percentage of m/z 190 and m/z 189, respectively, by the total ion count of the peak.
ND, not detected.

including T-Fuc, 2-Gal, 4-Glc, and 4,6-Glc with respect to the wild type and the single mutants (Table 2). However, there are two issues that confound efforts to draw simple conclusions from the results of the linkage analysis. First, some of the glycosyl linkages that are found in XyG, such as T-Fuc, 4-Glc, and 4,6-Glc, are also found in other polysaccharides present in the 4 N KOH fraction. Second, the linkage analysis data are presented on a relative percentage basis, which can be problematic to interpret because a decrease in one or more linkage species must be offset by a relative increase in other species. For example, the dramatic reduction of 4,6-Glc in the double mutant is offset by apparent increases in many other linkages.

To overcome these issues, we used 2-Xyl as an indicator of XyG via linkage analysis. However, because PMAA derivatives of 2- and 4-Xyl are symmetrical, they have the same retention time. To differentiate between 2- and 4-Xyl, one must rely upon the difference in the mass of the ions due to the deuterium introduced at the C-1 position during reduction (Figure 5A) (Carpita and Shea, 1989). Gas chromatography–mass spectrometry (GC-MS) results (Figure 5B) indicate that there is a >75% reduction in the relative amount of the ion that corresponds to 2-Xyl (mass-to-charge ratio [*m/z*] 190) with respect to the ion assigned to 4-Xyl (*m/z* 189) of the *xxt1 xxt2* double mutant compared with the wild type. The occurrence of *m/z* 190 in the 2- and 4-Xyl peak

indicates the presence of 2-Xyl. However, due to the presence of ^{13}C, 8.88% of *m/z* 189 will be measured at *m/z* 190 (Carpita and Shea, 1989). Therefore, we hypothesize that the majority of the *m/z* 190 ion counts in the 2- and 4-Xyl peak of the *xxt1 xxt2* double mutant originated from 4-Xyl and that there was a >90% reduction in 2-Xyl. These results show that the *xxt1 xxt2* double mutant has a significant reduction in the relative amounts of glycosyl linkages that can be assigned to XyG.

The *xxt1 xxt2* Mutant Lacks Driselase-Susceptible XyG

To further investigate the changes in XyG content, we used Driselase to digest crude cell wall preparations of wild-type, *xxt1*, *xxt2*, and *xxt1 xxt2* 7-d-old etiolated seedlings. This commercial enzyme preparation is comprised of a battery of exo- and endoglycosidases that will hydrolyze all major cell wall polysaccharides (Fry, 2000). However, Driselase lacks α-xylosidase activity; thus, digestion of XyG produces isoprimeverose (IP) [xylose-α-(1,6)-glucose], a disaccharide that has been used in past studies as a diagnostic indicator of XyG (Hayashi et al., 1981; Hayashi and Matsuda, 1981a, 1981b, 1981c; Hayashi and Maclachlan, 1984; Gordon and Maclachlan, 1989; Hayashi, 1989; Lorences and Fry, 1994; Gardner et al., 2002; Popper and Fry, 2003, 2005).
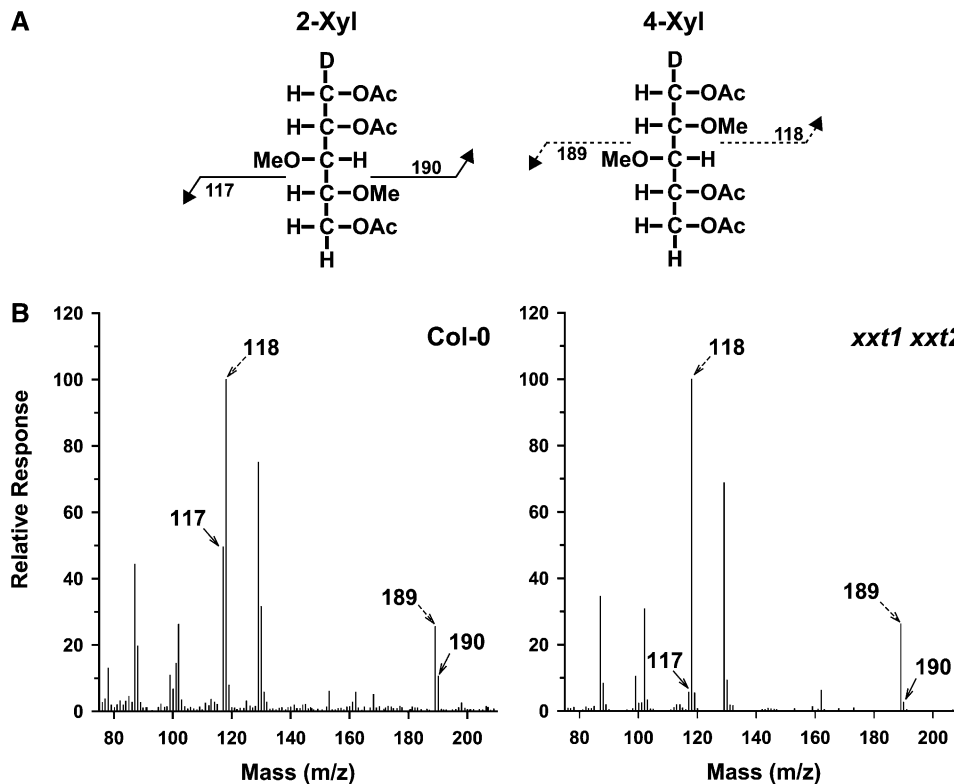

Figure 5. The *xxt1 xxt2* T-DNA Insertion Mutant has a 90% Decrease in 2-Xylose.

(A) A schematic of the primary fragmentation patterns and corresponding *m/z* of 2-Xyl and 4-Xyl PMAA derivatives.
(B) Electron-impact mass spectra of the 2-,4-Xyl peak from wild-type (Col-0) and *xxt1 xxt2* PMAA derivatives of crude cell wall preparations. Arrows denote the diagnostic fragmentation ions for 2-Xyl (solid arrows) and 4-Xyl (dashed arrows).

Table 3. Analysis of Driselase-Digested AIR Preparations of 7-d-Old Etiolated Seedlings

Genotype	IP[a] (μg mg^{-1} AIR)	Monosaccharide (μg mg^{-1} AIR) Composition of Driselase-Resistant Material[b]						
		Rhamnose	Fucose	Arabinose	Xylose	Mannose	Galactose	Glucose
Col-0	14.13 ± 0.07	3.38 ± 0.33	0.21 ± 0.05	7.29 ± 0.35	4.76 ± 0.36	1.32 ± 0.14	8.17 ± 0.71	21.23 ± 2.57
xxt1	12.69 ± 0.15*	3.43 ± 1.63	0.09 ± 0.10	6.58 ± 2.13	4.01 ± 1.27	1.33 ± 0.66	7.73 ± 2.78	19.00 ± 6.60
xxt2	11.19 ± 0.10*	3.47 ± 0.74	0.04 ± 0.05*	6.15 ± 2.11	3.92 ± 1.30	1.42 ± 0.15	6.31 ± 1.88	14.82 ± 6.89
xxt1 xxt2	ND*	2.78 ± 0.11	ND*	6.48 ± 0.33	3.91 ± 0.23	1.29 ± 0.09	4.73 ± 0.16*	15.88 ± 1.45

[a] HPAEC analysis of Driselase-susceptible AIRs.

[b] GC-MS analysis of monosaccharide alditol acetate derivatives released by Saeman hydrolysis of Driselase-resistant AIR.

Values are derived from $n = 3$ biological repetitions ± SD. *Statistically significant difference with respect to the wild type (Col-0; $P < 0.025$). Trace indicates trace amount detected but not quantified. ND, not detected.

HPAEC-PAD analysis of the Driselase-susceptible fraction indicated that, compared with the wild type, there was significantly less IP liberated from the crude cell wall preparations of all mutant lines. The *xxt1* and *xxt2* single mutants had reductions in IP content of 10.2 and 20.8%, respectively (Table 3). More interestingly, analysis of the products released by Driselase digestion of cell walls from the *xxt1 xxt2* double mutant indicated that there was no detectable IP released (Figure 6, Table 3).

To determine the limit of IP detection by HPAEC-PAD in these assays, 1:10 and 1:20 dilutions of Driselase-digested crude cell walls from wild-type etiolated seedlings were analyzed (see Supplemental Figure 4 online). Based upon the ability to easily detect IP in the 1:20 dilution of Driselase-digested wild-type cell walls and the lack of IP detected in the *xxt1 xxt2* double mutant, we concluded that the levels of XyG in the *xxt1 xxt2* mutant were down at least 95%, and probably more, when compared with wild-type plants.

To ensure that XyG from the T-DNA insertion mutants was not simply resistant to Driselase digestion, we subjected the Driselase-resistant material to Saeman hydrolysis, converted it to alditol acetates, and performed GC-MS analysis. We found no significant differences in the amounts of xylose, and most other sugars, present in the Driselase-resistant residues derived from wild-type and the mutant lines (Table 3).

Finally, to determine whether the lack of XyG in the *xxt1 xxt2* double mutant was due to the lack of *XXT1* and *XXT2* expression, we complemented *xxt1 xxt2* double mutants with either *35S$_{pro}$:XXT1* or *35S$_{pro}$:XXT2*. Crude cell wall preparations were made from individual complemented seedlings and digested with Driselase. Results from HPAEC-PAD analysis indicated the presence of IP in preparations derived from individual *xxt1 xxt2* double mutants complemented with either *35S$_{pro}$:XXT1* or *35S$_{pro}$:XXT2* (see Supplemental Figure 5 online). Combining these results with restoration of normal root hairs shows that disruption of both *XXT1* and *XXT2* expression caused the severe root hair phenotype and lack of detectable XyG in the *xxt1 xxt2* double mutant.

The *xxt2* and *xxt1 xxt2* T-DNA Insertion Mutants Have Reduced Stiffness and Ultimate Stress Compared with the Wild Type

Given that XyG is predicted to cross-link cellulose microfibrils to form a three-dimensional network that functions as the principal load-bearing structure of the plant primary cell wall, we wanted

to determine whether there was a difference in the mechanical properties of *xxt1*, *xxt2*, and *xxt1 xxt2* etiolated seedlings with respect to the wild type and the previously characterized *mur3-1* mutant (Ryden et al., 2003; Pena et al., 2004; Burgert, 2006). Etiolated seedling hypocotyls were chosen because they are
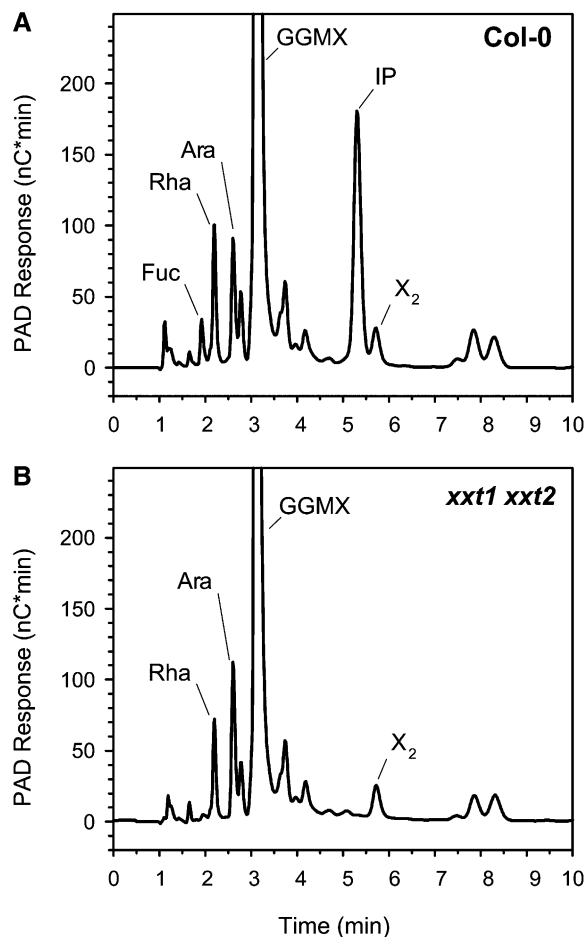
Figure 6. The *xxt1 xxt2* Double T-DNA Insertion Mutant Lacked Driselase-Susceptible XyG.

HPAEC analysis of Driselase-hydrolyzed AIR from wild-type (Col-0) **(A)** and *xxt1 xxt2* **(B)** etiolated seedlings. GGMX, peak comprised of galactose, glucose, mannose, and xylose; X_2, xylobiose.

composed mainly of expanding cells with primary cell walls and they have been used in past studies to measure the mechanical properties of *Arabidopsis* cell walls (Gendreau et al., 1997; Ryden et al., 2003; Pena et al., 2004; Burgert, 2006). Two mechanical parameters of the middle portion of the hypocotyls were determined: stiffness, which is defined as the ability of a material to resist elastic deformation; and ultimate stress, which is the measure of the mechanical stress a material can withstand before failure. Measurement of the cross-section area of the portion of each hypocotyl that was subjected to stress prior to mechanical testing indicated that the mutant lines had a significantly larger cross section than did wild-type plants (see Supplemental Figure 6 online). Results show that there were no significant differences in stiffness and ultimate stress between the wild type and *xxt1* (Figure 7), whereas *xxt2* and *xxt1 xxt2* mutants had significant reductions ($P < 0.001$) in stiffness and ultimate stress. Furthermore, there were no significant differences in these mechanical parameters between the *xxt2* single and the *xxt1 xxt2* double mutants. These results show that the reduction in XyG content has significant effects on the mechanical properties of *xxt2* and *xxt1 xxt2* mutant cell walls.

DISCUSSION

The finding that the *xxt1 xxt2* double mutant plants lacked detectable XyG is supported by the results from four independent strategies used to determine the presence of XyG. First, OLIMP and HPAEC-PAD analyses of crude cell wall preparations digested by XEG did not detect XyG-specific oligosaccharides. Second, there was a lack of labeling from all XyG-directed antibodies tested. Third, glycosyl linkage analysis showed a significant reduction in linkages associated with XyG. And fourth, HPAEC-PAD analysis of crude cell wall preparations digested

with Driselase did not detect IP. Therefore, we concluded that the *xxt1 xxt2* mutant lacks detectable XyG.

The *xxt1 xxt2* double mutant produced slightly smaller plants that had abnormal root hairs but normal trichomes. By contrast, the *mur2* and *mur3* XyG mutants have no defect in root hair morphology, but they do have a relatively subtle collapsed trichome papillae phenotype that is more severe in the *mur3* mutants (Vanzin et al., 2002; Madson et al., 2003). The root hair phenotype of the *xxt1 xxt2* double mutant demonstrates that XyG biosynthesis is important in these specialized cells that are undergoing tip growth, a process that has been shown to be sensitive to both environmental factors (Muller and Schmidt, 2004) and mutations (for examples, see Schiefelbein and Somerville [1990] and Baskin et al. [1992]). Indeed, there are several cell wall metabolism-related mutants that have aberrant root hair phenotypes, including mutations involving putative glycan synthases encoded by *CSL* genes, such as *KOJAK/CSLD3* from *Arabidopsis* (Favery et al., 2001; Wang et al., 2001) and *CSLD1* from rice (*Oryza sativa*; Kim et al., 2007); an *Arabidopsis* cell wall leucine-rich repeat extensin encoded by *LRX1* (Baumberger et al., 2001); an *Arabidopsis* UDP-D-Glc-4-epimerase (Seifert et al., 2002) involved in nucleotide sugar metabolism that is encoded by *REB1/RHD1* (Schiefelbein and Somerville, 1990; Baskin et al., 1992); and another putative XXT from *Arabidopsis* encoded by *XXT5* (formerly At *GT5*) (Zabotina et al., 2008).

To ensure that the root hair phenotype and the lack of detectable XyG in the *xxt1 xxt2* double mutant were the result of the disruption of *XXT1* and *XXT2* expression, we complemented the double mutant with either $35S_{pro}$:*XXT1* or $35S_{pro}$:*XXT2*. Results showed that the aberrant root hair phenotype was rescued and XyG content restored, as measured by the presence of IP released by Driselase. Therefore, based on the confluence of evidence from the reverse genetics study presented here and the heterologous
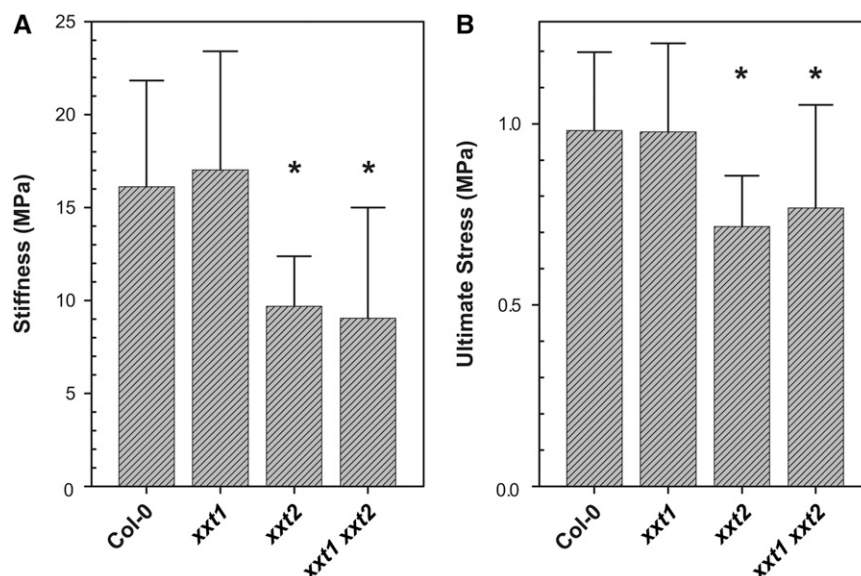

Figure 7. *xxt2* and *xxt1 xxt2* T-DNA Insertion Mutants Have a Reduction in Stiffness and Ultimate Stress.

Mechanical properties of 4-d-old etiolated hypocotyls of wild-type (Col-0; $n = 217$), *xxt1* ($n = 96$), *xxt2* ($n = 51$), and *xxt1 xxt2* ($n = 59$) T-DNA insertion mutants. Stiffness **(A)**; ultimate stress **(B)**. Asterisks denote statistically significant difference with respect to the wild type ($P < 0.001$). Error bars ± SD.

expression studies reported earlier (Faik et al., 2002; Cavalier and Keegstra, 2006; Fauré et al., 2007), we concluded that *XXT1* and *XXT2* encode XTs involved in XyG biosynthesis.

Although prior work has shown that *XXT1* and *XXT2* are closely related and encode proteins that have the same acceptor substrate requirements and produce identical reaction products when expressed in heterologous systems (Faik et al., 2002; Cavalier and Keegstra, 2006), it was unknown if these genes were genetically redundant. Results from the reverse genetics study presented here provide three lines of evidence to support the hypothesis that *XXT1* and *XXT2* are partially redundant genes (as defined by Briggs et al. [2006]). First, the modest reductions in XyG content of 10.2 and 20.8% in the *xxt1* and *xxt2* single mutants, respectively, was enhanced in the *xxt1 xxt2* double mutant. Second, the immunohistochemical analysis showed that there were differences in the distribution and intensity of immunofluorescent labeling with XyG-directed antibodies between the *xxt1* and *xxt2* single mutants. And third, the stiffness and ultimate stress parameters of the *xxt1* and *xxt2* single mutants were significantly different.

The functional genomics approach used here and in earlier studies (Faik et al., 2002; Cavalier and Keegstra, 2006) led to the identification of two XyG XTs, yet there are two issues regarding the XTs involved in XyG biosynthesis that have not been resolved. First, we do not have a complete understanding of which genes from CAZy family GT34 are required to produce the XXXG-repeating structure of *Arabidopsis* XyG in vivo. Similar to the requirement that at least two specific galactosyltransferases are needed for XyG biosynthesis (Madson et al., 2003; Li et al., 2004), there is evidence to support the hypothesis that two or more XyG XTs with different substrate specificities are required to synthesize the XXXG repeat. Evidence from a reverse genetics study by Zabotina et al. (2008) has shown that the protein encoded by *XXT5* is involved in XyG biosynthesis. The *xxt5* T-DNA insertion mutant has a decrease in XEG-released XXXG and XXFG and a corresponding increase in XXG and XXGG XyG oligosaccharides. Even though *XXT5* was expressed in the *xxt1 xxt2* double mutant (Figure 1), the double mutant lacked detectable XyG, which may be due to an epistatic effect whereby the activity of either XXT1 or XXT2 is required before XXT5 can act. Further work needs to be done for a better understanding of which members of CAZy family GT34 are required to produce the XXXG repeat.

The second important issue that needs to be resolved is whether the XTs form complexes with other XyG biosynthetic proteins, specifically XyG glucan synthase. One interpretation of the lack of past success in purifying XyG glucan synthase using conventional biochemical protein purification approaches is that the XyG glucan synthase and XyG XTs form complexes, in which the concomitant activities of these enzymes are needed to synthesize XyG (Ray, 1980; Hayashi and Matsuda, 1981b; Hayashi et al., 1988; Gordon and Maclachlan, 1989; Hayashi, 1989; Brummell et al., 1990; Perrin et al., 2001). However, the development of an acceptor-based XyG XT assay by Faik et al. (2002) showed that it is possible to measure XyG XT activity in detergent-solubilized pea microsomes independent of XyG glucan synthase activity, which was verified by heterologous expression studies of either *XXT1* or *XXT2* (Faik et al., 2002; Cavalier and Keegstra, 2006). Recently, using a heterologous expression

strategy, Cocuron et al. (2007) identified CSLC4 from *Arabidopsis* as a putative XyG glucan synthase. The coexpression of *CSLC4* and *XXT1* in *Pichia* cells did not produce any detectable XyG, which is not surprising because *Pichia* lacks UDP-Xyl. However, there was a significant increase in the degree of polymerization of β-glucan produced in *Pichia* lines coexpressing *CSLC4* and *XXT1* compared with β-glucan produced in *Pichia* lines expressing *CSLC4* alone. One interpretation of this observation is that CSLC4 and XXT1 interact, either directly or indirectly, to modulate the β-glucan length in *Pichia* cells (Cocuron et al., 2007). Therefore, it is likely that a membrane complex of XyG glucan synthase and XTs would be more efficient than solubilized enzymes at producing the observed XXXG repeating structure in planta. However, further work needs to be done to determine if a complex of β-glucan synthase and XXTs is required for XyG biosynthesis.

One significant ramification of the recovery of the *xxt1 xxt2* double mutant plants is the apparent contradiction between the lack of detectable XyG in this mutant and tether network models of the plant primary cell wall where the cellulose-XyG network is predicted to function as the main load-bearing component of the primary cell wall (Fry and Miller, 1989; Hayashi, 1989; McCann and Roberts, 1991; Passioura and Fry, 1992; Carpita and Gibeaut, 1993; Veytsman and Cosgrove, 1998; Somerville et al., 2004). These tether network models are exemplified by the sticky network model (Veytsman and Cosgrove, 1998; Cosgrove, 2000, 2001, 2005), in which XyG is predicted to hydrogen bond to cellulose microfibrils either to coat the cellulose microfibrils, preventing their association with nearby microfibrils and thereby forming large crystalline structures, or to cross-link adjacent cellulose microfibrils, thus forming a three-dimensional load-bearing network. In this model, selective modification of the cross-linking XyG primarily by the actions of expansins, or perhaps XyG endotransglucosylase/hydrolase, loosen the wall to allow the cellulose microfibrils to move apart relative to one another during turgor pressure–driven cell enlargement (Cosgrove, 2005). Although tether network models are certainly the most popular models, there is no direct evidence to support these models over others in which XyG is predicted to act as a spacer or an adapter (Cosgrove, 2001; Thompson, 2005; Burgert and Fratzl, 2007).

If the sticky network model can be described as approximating an isostress system (Thompson, 2005), whereby both cellulose and XyG bear the total load during cell wall expansion, then one could expect that a lack of detectable XyG would have catastrophic consequences for the integrity of the primary cell wall. The lack of a severe phenotype in the *xxt1 xxt2* double mutant can be interpreted as evidence that the primary cell wall cannot be accurately described as an isostress system; however, this observation does not provide any insight into how XyG content, or lack thereof, affects the mechanical properties of the primary cell wall. For that reason, we performed micromechanical stress tests on wild-type and mutant hypocotyls.

Although decreases in the stiffness and ultimate strength parameters of *xxt2* single and *xxt1 xxt2* double mutants is evidence that XyG contributes to the mechanical properties of the primary cell wall, we conclude that an isostress system cannot describe the mechanical properties of these mutants. This

conclusion is supported by the observation that the reduction in XyG content in these mutants caused no difference in mechanical parameters between wild-type and the *xxt1* single mutant and a modest reduction in these parameters in the *xxt2* single and *xxt1 xxt2* double mutants. Although the cell walls of these mutants cannot be described as an isostress system, they are also unlikely to be described as an isostrain system (Thompson, 2005; Burgert and Fratzl, 2007). An attractive alternative is an intermediate system where cellulose bears most of the load and XyG acts as a tether in longitudinal direction and a spacer (along with other cell wall components) in the lateral direction during anisotropic cell expansion (Burgert and Fratzl, 2007). However, there is no direct evidence to support the intermediate case, and further research is needed to understand how the composition and arrangement of the cell wall components affect the mechanical properties of the primary cell wall.

There are two confounding points to consider from the results of the micromechanical stress tests. First, while there were no significant differences in stiffness and ultimate stress measurements between wild-type and the *xxt1* single mutant hypocotyls, the *xxt2* single mutant hypocotyls had significant decreases in both of these mechanical parameters. We interpret these results and the larger decrease in XyG content of the *xxt2* single mutant as evidence to support the hypothesis that there exists a threshold level of XyG that is required for normal function. Second, the finding that there were no significant differences in the stiffness and ultimate stress measurements between the *xxt2* single and *xxt1 xxt2* double mutants should be interpreted with caution because it is unknown how the *xxt1 xxt2* double mutant adapts to the lack of detectable XyG. Indeed, several possible scenarios can be offered to explain why the *xxt1 xxt2* double mutant is viable without detectable XyG.

First, it is possible that the *xxt1 xxt2* mutant has XyG with a significantly lower Xyl:Glc ratio than the characteristic 3:4 found in *Arabidopsis* XyG. This type of XyG could be formed by the action of another member of CAZy family GT34 that, because of the lack of *XXT1* and *XXT2* expression, is inefficient at adding a xylosyl residue to the β-glucan backbone. Thus, the abnormal XyG, although not functioning in the same capacity as typical XyG, would allow the plant to survive. This aberrant XyG would unlikely be detected by either OLIMP or immunohistochemical analyses due to the specificity of XEG and the XyG-specific antibodies, respectively. However, the inability to detect even low levels of IP in the *xxt1 xxt2* double mutant argues against this scenario. A second possibility is that the β-glucan backbone synthesized by XyG glucan synthase is being used as a cell wall cross-linking glucan. Indeed, evidence from glycosyl residue composition analysis of the *xxt1 xxt2* double mutant provides some support for this hypothesis in that the decrease in TFA-released Xyl was not matched by a corresponding decrease in TFA-released Glc (Table 1). Unfortunately, this hypothesis is difficult to test because we lack the ability to distinguish unsubstituted XyG β-glucan backbone from amorphous cellulose. In addition, it is difficult to understand how the unsubstituted β-glucan chain can be maintained in a soluble form while it is transported from the Golgi to the cell wall. It is also difficult to imagine how the β-glucan chain can be reorganized in the cell wall given that it would not be a substrate for the XET that

reorganizes XyG in the wall. Despite these difficulties, we cannot eliminate this interesting possibility. Still a third possibility is that other cell wall components are compensating for the deficiency in XyG. However, immunohistochemical and glycosyl residue linkage analyses did not reveal any obvious candidates, and results from phloroglucinol staining of 7-d-old seedlings did not show any evidence of ectopic lignification.

It is also possible that the *xxt1 xxt2* double mutant adapts to the lack of detectable XyG, not by increasing the amount of a particular cell wall component, but by modifying how the remaining components are organized within the primary cell wall. This type of compensation mechanism would certainly not be detected by either the biochemical analyses or the limited range of non-XyG directed antibodies used in this study. One potential mechanism is to modulate pectin cross-linking. Perhaps there is a higher degree of either homogalacturonan cross-linking via calcium bridges, which results in more rigid pectic gels that are thought to strengthen the cell wall (Willats et al., 2001), or RG-II dimerization via borate bridges, which has been shown to be an important component of the mechanical properties of the cell wall (Ryden et al., 2003). Finally, it is possible that there is no compensation mechanism and that the *xxt1 xxt2* double mutant can exist only under a limited set of growth conditions used in the lab. However, further work needs to be done to understand how the *xxt1 xxt2* double mutant adjusts to the lack of detectable XyG.

In conclusion, results from this reverse genetics study, in conjunction with results from the heterologous expression studies (Faik et al., 2002; Cavalier and Keegstra, 2006), demonstrate that *XXT1* and *XXT2* encode XyG XTs that are required for XyG biosynthesis. We have also shown that the *xxt1* and *xxt2* single mutants had a modest reduction in XyG and, surprisingly, that the *xxt1 xxt2* double mutant lacks detectable XyG. Yet, all three mutants lacked a significant gross morphological phenotype and were viable under laboratory conditions. Furthermore, we showed that the reduction of XyG content in the *xxt2* single mutant and the lack of detectable XyG in the *xxt1 xxt2* double mutant caused significant reductions in the stiffness and ultimate strength parameters of these mutants. Although our results presented here provide evidence that challenges the conventional models of the primary cell wall, further work is needed to understand how XyG functions in the primary cell wall. The *xxt1* and *xxt2* single and the *xxt1 xxt2* double mutant plants described here will provide a valuable resource for investigation of the structure-function relationship between components of the plant primary cell wall.

METHODS

Clones, Plant Material, Growth Conditions, and Genetic Analysis

Faik et al. (2002) and Cavalier and Keegstra (2006) showed in vitro that *XT1* and *XT2* from *Arabidopsis* encode XTs that are postulated to be involved in XyG biosynthesis. In this study, we have provided evidence that *XT1* and *XT2* from *Arabidopsis* encode XTs involved in xyloglucan biosynthesis in vivo. Therefore, to indicate that these genes are XyG XTs and to satisfy the gene nomenclature standards adopted by the *Arabidopsis* community (Meinke and Koornneef, 1997), we have changed the names *XT1* and *XT2* to *xyloglucan xylosyltransferse1* (*XXT1*) and *XXT2*, respectively.

The cDNA clones for *XXT1* and *XXT2* were obtained from the ABRC. *Arabidopsis thaliana* (Col-0) T-DNA insertion mutants were obtained from either the Salk collection (Alonso et al., 2003) through the ABRC or the SAIL collection from Syngenta (Sessions et al., 2002) and grown on either soil or agar plates according to the conditions described by Constan et al. (2004). For biochemical analysis, microtensile testing of hypocotyls, and RT-PCR, etiolated seedlings were grown according to Lerouxel et al. (2002) and Obel et al. (2006).

For genetic analysis, homozygous *xxt1* (SAIL_785-E02) and *xxt2* (Salk_101308) T-DNA insertion lines were isolated using PCR with gene- and T-DNA–specific primers (see Supplemental Table 2 online). The *xxt1 xxt2* double knockout line was generated by crossing homozygous *xxt1* (male) and *xxt2* (female) mutants. The F1 generation was allowed to self-fertilize, and a PCR screen using gene- and T-DNA–specific primers identified two *xxt1 xxt2* double knockout plants from a population of 189 F2 generation plants.

All T-DNA knockout and Col lines were analyzed by RT-PCR to determine the presence of *XXT1* and *XXT2* transcripts. Ubiquitin (UBQ10) and, in the case of the *xxt1 xxt2* double knockout line, *XXT5*, were used as controls. Total RNA was isolated from three independent pools of 7-d-old seedlings using the RNeasy kit (Qiagen) with two sequential DNase treatments. The RNA was transcribed into cDNA with Superscript II (Invitrogen) reverse transcriptase. PCR was performed on the cDNA template with JumpStart REDTaq ReadyMade PCR mix (Sigma-Aldrich) at 35 cycles of 94°C for 45 s, 55°C for 1 min, 72°C for 2 min, and a final extension at 72°C for 5 min. The primer sequences are presented in Supplemental Table 2 online. RT-PCR products were separated on a 1% agarose gel containing 0.005% ethidium bromide.

The *xxt1 xxt2* double T-DNA insertion mutant is available from the ABRC (seed stock number CS16349).

Preparation of Cell Wall AIRs

Cell wall AIRs were generated from etiolated seedlings by methods adapted from Fry (2000) and Lerouxel et al. (2002). Briefly, etiolated seedlings were harvested directly into 70% (v/v) ethanol, and the tissue was ground in a Potter homogenizer. The samples were incubated for 1 h at 65°C and centrifuged; the pellet was washed twice with 70% ethanol and extracted with a mixture of chloroform and methanol (1:1). The pellet was suspended in acetone, transferred to a preweighed 1.5-mL screw-cap microtube (Sarstedt), and air-dried overnight. The AIR was weighed, ball-milled (Retsch) for 5 min, and suspended in water to a final concentration of 10 mg mL^{-1}.

OLIMP

AIR was generated from wild-type, *xxt1*, *xxt2*, and *xxt1 xxt2* 4-d-old etiolated seedlings and analyzed by OLIMP according to previously published methods by Lerouxel et al. (2002) and Obel et al. (2006). The AIR from a single hypocotyl ($\sim$20 μg) was suspended in 50 μL of 100 mM ammonium formate buffer, pH 4.5, containing 0.02 units of purified recombinant XEG (EC 3.2.1.151) (Pauly et al., 1999b) and incubated at 37°C for 18 h. The reactions were centrifuged to pellet undigested AIR, and the supernatant containing soluble XGOs was removed and dried down. The XGOs were dissolved in 6 μL of water containing $\sim$10 beads of Bio-Rex MSZ 501(D) resin (Bio-Rad) to remove buffer salts (Obel et al., 2006). One microliter of the oligosaccharide solution was spotted onto a MALDI-TOF sample plate containing vacuum-dried 2,5-dihydroxybenzoic acid (10 mg mL^{-1}; 1 μL per well) and crystallized under vacuum. Spectra samples were analyzed on a Voyager DE-Pro MALDI-TOF-MS instrument (Applied Biosystems) in positive reflectron mode with an acceleration voltage of 20 kV and an extraction delay time of 350 ns. Custom PERL-based software (Lerouxel et al., 2002) was used to calculate the relative area of each XGO ion peak and to perform pairwise comparisons and Student's *t* tests of the respective XGO peak areas from mutant and wild-type samples.

Cell Wall–Directed Monoclonal Antibodies

All monoclonal antibodies against plant cell wall carbohydrate epitopes were in the form of hybridoma supernatants and were used undiluted. The CCRC and JIM antibodies used in this study were from laboratory stocks and are available from CarboSource (http://cell.ccrc.uga.edu/$\sim$carbosource/CSS_home.html). Although CCRC-M1 was raised against sycamore maple (*Acer pseudoplantanus*) RG-I, an antigen that it recognizes weakly in vitro, it has been shown to bind strongly to an α-L-Fucp(1→2)-β-D-Galp epitope found in dicot XyG (Puhlmann et al., 1994). CCRC-M39, CCRC-M58, CCRC-M87, and CCRC-M89 are newly generated monoclonal antibodies that bind to XyG epitopes distinct from each other and from the epitope recognized by CCRC-M1 (Z. Popper, T. Bootten, R. Jia, S. Tuomivaara, A.G. Swennes, W.S. York, and M.G. Hahn, unpublished data). CCRC-M2 binds to a developmentally regulated RG-I epitope (Puhlmann et al., 1994; Freshour et al., 1996). CCRC-M34 and CCRC-M38 were generated from mice immunized with *Arabidopsis* seed mucilage (T. Bootten, Z. Popper, and M.G. Hahn, unpublished data). CCRC-M34 appears to bind to an as yet uncharacterized (probably methylesterified) epitope in pectins, and CCRC-M38 binds to unesterified homogalacturonan (R. Jia, C. Deng, T. Bootten, Z. Popper, W.S. York, M.A. O'Neill, and M.G. Hahn, unpublished data). JIM5 and JIM7 bind to homogalacturonan epitopes containing different densities and patterns of methylesterification (Knox et al., 1990; Willats et al., 2000; Clausen et al., 2003). JIM13 binds to a GlcA-containing epitope present in arabinogalactan structures (Yates et al., 1996). JIM19 was generated against *Pisum sativum* guard cell protoplasts (Knox et al., 1995) and binds to various exudate gums, seed mucilages, and RG-I preparations (A.G. Swennes and M.G. Hahn, unpublished data). The xylan-directed antibodies LM10 and LM11 (McCartney et al., 2005) were obtained from PlantProbes.

Tissue Fixation

Four-day-old seedlings, with roots 10 to 12 mm in length, were fixed for 2.5 h in fixing solution composed of 1.6% (w/v) paraformaldehyde and 0.2% (w/v) glutaraldehyde in 25 mM sodium phosphate, pH 7.1. Tissue was rinsed with buffer twice for 15 min each, with water twice for 15 min each, and dehydrated at room temp through a graded ethanol series (20-35-50-62-75-85-95-100-100-100% [v/v] ethanol) for 30 min at each step. The dehydrated tissue was moved to 4°C and gradually infiltrated with a graded series of cold LR White embedding resin (Ted Pella) (33 and 66% resin in 100% ethanol, 24 h each, followed by three changes of 100% resin, also 24 h each). The infiltrated tissue was transferred to gelatin capsules containing 100% resin for embedding, and resin was polymerized by exposing the capsules to 365-nm UV light at 4°C for 48 h.

Immunohistochemistry

Semithin sections (250 nm) were cut with a Reichert-Jung Ultracut E ultramicrotome and mounted on glass microslides previously coated with 0.5% (w/v) gelatin and 0.05% (w/v) chromium potassium sulfate (chrom-alum; Fisher). Immunolabeling was performed at room temperature, applying (and removing) a series of $\sim$10-μL droplets of the appropriate reagents to the sections described as follows: Nonspecific antibody binding sites on the sections were blocked by incubating the sections for 75 min with 3% (w/v) nonfat dry skim milk in 10 mM potassium phosphate, pH 7.1, containing 0.5 M NaCl (potassium phosphate buffered saline, KPBS). The sections were then rinsed with KPBS for 5 min and incubated with undiluted hybridoma supernatant for 120 to 150 min. Sections were then washed with KPBS three times for 5 min each,

followed by secondary antibody (goat anti-mouse conjugated to Alexa-fluor 488; Invitrogen A11001) diluted 1:100 in KPBS for 90 to 120 min. Sections were then washed with KPBS for 5 min, then with distilled water for 5 min. Prior to applying a cover slip, PPD mounting media (90% [v/v] glycerol, containing 0.1% [v/v] paraphenylenediamine, 0.01 M potassium phosphate, pH 9.0, and 0.15 M NaCl) was applied. Cover slips were sealed to the glass slides with nail polish. Root sections were examined by light and immunofluorescence microscopy on an Axioscop microscope (Carl Zeiss) equipped with differential interference contrast and epifluorescence optics. Images were captured with a Nikon DS-L1 camera control unit with a DS-5M camera head and processed using Photoshop.

Glycosyl Residue Composition Analysis of Crude Cell Wall Preparations

Alditol acetate derivatives of neutral sugars from TFA-hydrolyzed AIR were produced as described by York et al. (1985). Approximately 1 mg of AIR from either 7-d-old etiolated seedlings or suspension-cultured cells and 10 μg of *myo*-inositol (internal standard) were hydrolyzed with 250 μL of 2.0 N TFA at 121°C for 90 min. After the reaction vessels were allowed to cool, the tubes were centrifuged to pellet TFA-resistant material. The supernatant containing TFA-hydrolyzed material was removed to a new tube, and the TFA-resistant material was twice suspended in 500 μL of water and centrifuged to remove residual TFA-hydrolyzed material.

The TFA-resistant material was lyophilized and further hydrolyzed by the Saeman method according to Selvendran et al. (1979) and neutralized according to Hough et al. (1972), with modifications. TFA-resistant material was suspended in 72% sulfuric acid containing 10 μg *myo*-inositol and incubated at room temperature for 1 h with intermittent vortexing. The samples were diluted with water to 1 M sulfuric acid and incubated at 100°C for 3 h. After the samples were allowed to cool, they were neutralized and extracted with 1 mL of 20% (v/v) dioctylamine in chloroform. The samples were vortexed, the organic and water phases were separated by centrifugation, and the organic phase was removed. The aqueous phase was extracted with 1 mL of 20% (v/v) dioctylamine in chloroform for a total of four times followed by four extractions with 1 mL of chloroform. One hundred microliters of the aqueous phase was used in the preparation of alditol acetates.

The TFA- and Saeman-hydrolyzed materials were dried down under a stream of nitrogen. Samples were suspended in 300 μL of 2-propanol and dried under a stream of nitrogen followed by an additional evaporation with 300 μL of 2-propanol. For the reduction of glycoses to corresponding alditols, each sample was suspended in 100 μL of 1 M NH$_4$OH by sonication followed by the addition of 100 μL of NaBH$_4$ solution (20 mg mL^{-1} dissolved in 1 M NH$_4$OH). Samples were vortexed and incubated at room temperature for 90 min. Reduction was terminated by the addition of 30 μL of glacial acetic acid, and the samples were vortexed and evaporated to dryness under a stream of nitrogen. The reduced samples were suspended with 200 μL of methanol/glacial acetic acid (9:1) and dried under a stream of nitrogen. Two additional evaporations with methanol/glacial acetic acid (9:1) followed by four evaporations with 200 μL of methanol were performed. For acetylation, the reduced samples were suspended in 100 μL of acetic anhydride and 100 μL of pyridine and incubated at 121°C for 20 min. Acetylation reactions evaporated to dryness under a stream of nitrogen at room temperature, followed by two additional evaporations with 200 μL of toluene. The samples were suspended in 4 mL of water and 1 mL of methylenechloride, vortexed, and centrifuged. The water phase was removed and the organic phase was extracted a second time with 4 mL of water, as described above. The methylenechloride phase containing the per-*O*-acetylated alditols was dried under a stream of nitrogen at room temperature, suspended in acetone, and analyzed using an Agilent 6890 Series GC system equipped

with a 5975B inert XL MSD and an SP-2380 fused silica capillary column (30 m $\times$ 0.25 mm i.d. x 20 μm film thickness; Supelco).

For determining galacturonic and glucuronic acid content, TFA hydrolyzed material was suspended in water and analyzed by HPAEC (for instrumentation, see below) under conditions described by Obro et al. (2004).

Glycosyl Residue Linkage Analysis

For the production of PMAA derivatives for glycosyl residue linkage analysis, 0.50 to 0.75 mg of AIR was methylated according to the NaOH method developed by Ciucanu and Kerek (1984) with modifications by Ciucanu (2006). Methylated samples were hydrolyzed with TFA, reduced with NaBD$_4$, and acetylated as described above. The PMAA derivatives were analyzed on an Agilent 6890 Series GC system equipped with a 5975B inert XL MSD and an SP-2380 fused silica capillary column (30 m $\times$ 0.25 mm i.d. x 20 μm film thickness; Supelco). Glycosyl residue linkages were assigned based on the mass spectra and retention times of known standards. Although unambiguously assigned glycosyl linkages were reported, there were no apparent differences in unassigned glycosyl linkages between Col-0 and the mutants. With the exception of the 2-Xyl and 4-Xyl, the glycosyl residues are expressed as a percentage of the total peak areas. The 2-Xyl peak percentage was calculated by multiplying the peak area by the ion count of *m/z* 190 divided by the total ion counts of *m/z* 189 and *m/z* 190. The 4-Xyl peak percentage was calculated by multiplying the peak area by the ion count of *m/z* 189 divided by the total ion counts of *m/z* 189 and *m/z* 190. Finally, see Carpita and Shea (1989) for a discussion about the caveats of interpreting data derived from linkage analysis.

Driselase Digestion of Crude Cell Wall Preparations and HPAEC Analysis

Driselase (Sigma-Aldrich) was partially purified according to Fry (2000). One milligram of AIR from either 7-d-old etiolated seedlings or suspension-cultured cell lines of wild-type, *xxt1*, *xxt2*, and *xxt1 xxt2* was digested with Driselase and processed according to Gardner et al. (2002). For HPAEC analysis, each sample was suspended in water, passed through a 22-μm syringe filter, and analyzed on an ICS-3000 ion chromatography machine (Dionex) equipped with a CarboPac PA20 anion exchange column and electrochemical detector. Mono- and disaccharides were eluted from the column at a flow rate of 0.5 mL min^{-1} from 0 to 20 min under 125 mM NaOH isocratic conditions. The column was washed and reequilibrated under the following conditions: 20 to 35 min, 125 to 800 mM NaOH gradient; 35 to 40 min, 800 mM NaOH; 40 to 60 min, 125 mM NaOH. Sugars were detected with pulsed amperometric detection. Under these conditions Driselase-released neutral monosaccharides, IP, and xylobiose elute in the first 10 min; therefore only the first 10 min of each HPAEC run is shown. There were no differences between the chromatograms of Col-0 and mutants over the remaining 50 min of the HPAEC run.

Microtesile Testing of Hypocotyls

Four-day-old etiolated *Arabidopsis* hypocotyls were tested in a micro-tensile apparatus equipped with a sensitive load cell of 500 mN maximum capacity, originally designed to test individual wood fibers (Burgert et al., 2003). Custom-designed foliar frames were mounted onto a microtensile apparatus via a pinhole assembly. Individual hypocotyls were glued onto a foliar frame with a span length of ~2.5 mm in a stepwise combination of rapid cyanoacrylate adhesive and ESPE Ketac Cem Aplicap glass ionomer luting cement (3M). Video extensometry was used to measure the displacement of black lines drawn on the foliar frame to get an

accurate measurement of hypocotyl elongation. For further details about the microtensile testing instrumentation, see Burgert et al. (2003).

Hypocotyls were tested at room temperature at a strain rate of 15 μm s^{-1}. To avoid drying while testing, water vapor was constantly applied to the specimens. Stress-strain curves were calculated from force and elongation measurements. Strain is defined as the elongation of the hypocotyl divided by its initial span length. Stress is defined as the applied force divided by the area of the loaded cross section, which was determined by measuring the diameter of the hypocotyls (assuming the hypocotyls were cylindrical) under a microscope prior to testing. To compare the mechanical performance of the wild-type and the mutant hypocotyls directly, we calculated stiffness (slope of the stress-strain curve after initial adjustment of the hypocotyl) and ultimate stress. Stiffness is a measure of the ability of the material to resist elastic deformation, and ultimate stress is a measure of the mechanical stress a material can withstand before failure.

Complementation of the *xxt1 xxt2* Double Mutant

Gateway technology (Invitrogen) was used to make 35S$_{pro}$:*XXT1* and 35S$_{pro}$:*XXT2* constructs. Coding sequences for *XXT1* and *XXT2* were directionally cloned (using primers listed in Supplemental Table 2 online) into pENTR/D-TOPO vector (Invitrogen) according to the manufacturer's instructions (Cavalier and Keegstra, 2006). These constructs were moved into the pH2GW7 plant transformation vector (Karimi et al., 2002) via 18-h Clonase reactions. Plants were transformed by the vacuum infiltration method described by Bechtold and Bouchez (1994), with modifications by Hoof and Green (1996). Complementation was verified by the lack of the *xxt1 xxt2* double mutant root hair phenotype and the presence of IP in Driselase-digested crude cell wall preparations, as described above.

Accession Numbers

Sequence data from this article can be found in the Arabidopsis Genome Initiative or GenBank/EMBL data libraries under the following accession numbers: At3g28180 (*CSLC4*); At3g62720 (*XXT1*); U14458 (*XXT1* full-length *cDNA clone*); At4g02500 (*XXT2*); U25215 (*XXT2* full-length cDNA clone); At1g74380 (*XXT5*); and At4g05320 (*UBQ10*).

Supplemental Data

The following materials are available in the online version of this article.

Supplemental Figure 1. Wild-Type and *xxt1 xxt2* Plants.

Supplemental Figure 2. Immunofluorescent Labeling of Wild-Type and Mutant Roots Using Non-XyG-Directed Antibodies.

Supplemental Figure 3. Sugar Composition Analysis of T-DNA Insertion Mutants.

Supplemental Figure 4. HPAEC-PAD Analysis of Dilutions of Wild-Type Driselase-Digested Crude Cell Wall Preparations.

Supplemental Figure 5. HPAEC-PAD Analysis of Driselase-Digested Crude Cell Wall Preparations from Wild-Type and *xxt1 xxt2* Double Mutant Plants Complemented with Either 35S$_{pro}$:*XXT1* or 35S$_{pro}$:*XXT2*.

Supplemental Figure 6. Hypocotyl Cross-Section Area of T-DNA Insertion Mutants.

Supplemental Table 1. Xyloglucan-Directed Antibodies Used in This Study.

Supplemental Table 2. Primer Sequences Used for Genetic Analysis and Complementation.

REFERENCES

Alonso, J.M., et al. (2003). Genome-wide insertional mutagenesis of *Arabidopsis thaliana.* Science **301:** 653–657.

Baskin, T., Betzner, A., Hoggart, R., Cork, A., and Williamson, R. (1992). Root morphology mutants in *Arabidopsis thaliana.* J. Plant Funct. Biol. **19:** 427–437.

Baumberger, N., Ringli, C., and Keller, B. (2001). The chimeric leucine-rich repeat/extensin cell wall protein LRX1 is required for root hair morphogenesis in *Arabidopsis thaliana.* Genes Dev. **15:** 1128–1139.

Bechtold, N., and Bouchez, D. (1994). *In planta Agrobacterium-*mediated gene transfer by infiltration of adult *Arabidopsis thaliana* plants by vacuum infiltration. In Gene Transfer to Plants, I. Potrykus and G. Spangenberg, eds (Berlin: Springer-Verlag), pp. 19–23.

Briggs, G.C., Osmont, K.S., Shindo, C., Sibout, R., and Hardtke, C.S. (2006). Unequal genetic redundancies in *Arabidopsis* - A neglected phenomenon? Trends Plant Sci. **11:** 492–498.

Brummell, D.A., Camirand, A., and Maclachlan, G. (1990). Differential distribution of xyloglucan glycosyl transferases in pea Golgi dictyosomes and secretory vesicles. J. Cell Sci. **96:** 705–710.

Burgert, I. (2006). Exploring the micromechanical design of plant cell walls. Am. J. Bot. **93:** 1391–1401.

Burgert, I., and Fratzl, P. (2007). Mechanics of the expanding cell wall. In The Expanding Cell, J.-P. Verbelen and K. Vissenberg, eds (Berlin: Springer-Verlag), pp. 191–215.

Burgert, I., Fruhmann, K., Keckes, J., Fratzl, P., and Stanzl-Tschegg, S. (2003). Microtensile testing of wood fibers combined with video extensometry for efficient strain detection. Holzforschung **57:** 661–664.

Campbell, J., Davies, G., Bulone, V., and Henrissat, B. (1997). A classification of nucleotide-diphospho-sugar gylcosyltransferases based on amino acid sequence similarities. Biochem. J. **326:** 929–939.

Carpita, N.C., and Gibeaut, D.M. (1993). Structural models of primary cell walls in flowering plants: Consistency of molecular structure with the physical properties of the walls during growth. Plant J. **3:** 1–30.

Carpita, N., and McCann, M. (2000). The cell wall. In Biochemistry and Molecular Biology of Plants, B.B. Buchanan, G. Wilhelm, and R.L. Jones, eds (Rockville, MD: American Society of Plant Physiologists), pp. 52–108.

Carpita, N.C., and Shea, E.M. (1989). Linkage structure of carbohydrates by gas chromatography-mass spectrometry (GC-MS) of partially methylated alditol acetates. In Analysis of Carbohydrates by GLC and MS, C.J. Biermann and G.D. McGinnis, eds (Baton Raton, FL: CRC Press), pp. 157–216.

Cavalier, D.M., and Keegstra, K. (2006). Two xyloglucan xylosyltransferases catalyze the addition of multiple xylosyl residues to cellohexaose. J. Biol. Chem. **281:** 34197–34207.

Ciucanu, I. (2006). Per-*O*-methylation reaction for structural analysis of carbohydrates by mass spectrometry. Anal. Chim. Acta **576:** 147–155.

Ciucanu, I., and Kerek, F. (1984). A simple and rapid method for the permethylation of carbohydrates. Carbohydr. Res. **131:** 209–217.

Clausen, M.H., Willats, W.G.T., and Knox, J.P. (2003). Synthetic methyl hexagalacturonate hapten inhibitors of anti-homogalacturonan monoclonal antibodies lm7, jim5 and jim7. Carbohydr. Res. **338:** 1797–1800.

Cocuron, J.-C., Lerouxel, O., Drakakaki, G., Alonso, A.P., Liepman, A.H., Keegstra, K., Raikhel, N., and Wilkerson, C.G. (2007). A gene from the cellulose synthase-like C family encodes a β-1,4 glucan synthase. Proc. Natl. Acad. Sci. USA **104:** 8550–8555.

Constan, D., Froehlich, J.E., Rangarajan, S., and Keegstra, K. (2004). A stromal Hsp100 protein is required for normal chloroplast development and function in *Arabidopsis.* Plant Physiol. **136:** 3605–3615.

Cosgrove, D.J. (2000). Expansive growth of plant cell walls. Plant Physiol. Biochem. **38:** 109–124.

Cosgrove, D.J. (2001). Wall structure and wall loosening. A look backwards and forwards. Plant Physiol. **125:** 131–134.

Cosgrove, D.J. (2005). Growth of the plant cell wall. Nat. Rev. Mol. Cell Biol. **6:** 850–861.

Coutinho, P.M., Deleury, E., Davies, G.J., and Henrissat, B. (2003). An evolving hierarchical family classification for glycosyltransferases. J. Mol. Biol. **328:** 307–317.

Edwards, M.E., Dickson, C.A., Chengappa, S., Sidebottom, C., Gidley, M.J., and Reid, J.S. (1999). Molecular characterisation of a membrane-bound galactosyltransferase of plant cell wall matrix polysaccharide biosynthesis. Plant J. **19:** 691–697.

Faik, A., Bar-Peled, M., DeRocher, A.E., Zeng, W., Perrin, R.M., Wilkerson, C., Raikhel, N.V., and Keegstra, K. (2000). Biochemical characterization and molecular cloning of an α-1,2-fucosyltransferase that catalyzes the last step of cell wall xyloglucan biosynthesis in pea. J. Biol. Chem. **275:** 15082–15089.

Faik, A., Price, N.J., Raikhel, N.V., and Keegstra, K. (2002). An *Arabidopsis* gene encoding an α-xylosyltransferase involved in xyloglucan biosynthesis. Proc. Natl. Acad. Sci. USA **99:** 7797–7802.

Fauré, R., Cavalier, D.M., Keegstra, K., Cottaz, S., and Driguez, H. (2007). Glycosynthase-assisted synthesis of xylo-gluco-oligosaccharide probes for α-xylosyltransferases. Eur. J. Org. Chem. **2007:** 4313–4319.

Favery, B., Ryan, E., Foreman, J., Linstead, P., Boudonck, K., Steer, M., Shaw, P., and Dolan, L. (2001). KOJAK encodes a cellulose synthase-like protein required for root hair cell morphogenesis in *Arabidopsis.* Genes Dev. **15:** 79–89.

Freshour, G., Clay, R.P., Fuller, M.S., Albersheim, P., Darvill, A.G., and Hahn, M.G. (1996). Developmental and tissue-specific structural alterations of the cell-wall polysaccharides of *Arabidopsis thaliana* roots. Plant Physiol. **110:** 1413–1429.

Fry, S., and Miller, J. (1989). Towards a working model of the growing plant cell wall. Phenolic cross-linking reactions in the primary cell walls of dicotyledons. In Plant Cell Wall Polymers: Biogenesis and Biodegradation, N. Lewis and M. Paice, eds (Washington, DC: American Chemical Society), pp. 33–46.

Fry, S.C. (1989). The structure and functions of xyloglucan. J. Exp. Bot. **40:** 1–11.

Fry, S.C. (2000). The Growing Plant Cell Wall: Chemical and Metabolic Analysis. (Caldwell, NJ: The Blackburn Press).

Fry, S.C., et al. (1993). An unambigous nomenclature for xyloglucan-derived oligosaccharides. Physiol. Plant. **89:** 1–3.

Gardner, S.L., Burrell, M.M., and Fry, S.C. (2002). Screening of *Arabidopsis thaliana* stems for variation in cell wall polysaccharides. Phytochemistry. **60:** 241–254.

Gendreau, E., Traas, J., Desnos, T., Grandjean, O., Caboche, M., and Hofte, H. (1997). Cellular basis of hypocotyl growth in *Arabidopsis thaliana.* Plant Physiol. **114:** 295–305.

Gordon, R., and Maclachlan, G. (1989). Incorporation of UDP-[^{14}C]glucose into xyloglucan by pea membranes. Plant Physiol. **91:** 373–378.

Ha, M.A., Apperley, D.C., and Jarvis, M.C. (1997). Molecular rigidity in dry and hydrated onion cell walls. Plant Physiol. **115:** 593–598.

Hayashi, T. (1989). Xyloglucans in the primary cell wall. Annu. Rev. Plant Physiol. Plant Mol. Biol. **40:** 139–168.

Hayashi, T., Kato, Y., and Matsuda, K. (1981). Biosynthesis of xyloglucan in suspension-cultured soybean cells. An assay method for xyloglucan xylosyltransferase and attempted synthesis of xyloglucan from UDP-D-xylose. J. Biochem. **89:** 325–328.

Hayashi, T., Koyama, T., and Matsuda, K. (1988). Formation of UDP-xylose and xyloglucan in soybean Golgi membranes. Plant Physiol. **87:** 341–345.

Hayashi, T., and Maclachlan, G. (1984). Pea xyloglucan and cellulose. I. Macromolecular organization. Plant Physiol. **75:** 596–604.

Hayashi, T., and Matsuda, K. (1981a). Biosynthesis of xyloglucan in suspension-cultured soybean cells. Evidence that the enzyme system of xyloglucan synthesis does not contain β-1,4-glucan 4-β-D-glucosyltransferase. Plant Cell Physiol. **22:** 1571–1584.

Hayashi, T., and Matsuda, K. (1981b). Biosynthesis of xyloglucan in suspension-cultured soybean cells. Occurrence and some properties of xyloglucan 4-β-D-glucosyltransferase and 6-α-D-xylosyltransferase. J. Biol. Chem. **256:** 11117–11122.

Hayashi, T., and Matsuda, K. (1981c). Biosynthesis of xyloglucan in suspension-cultured soybean cells. Synthesis of xyloglucan from UDP-glucose and UDP-xylose in the cell-free system. Plant Cell Physiol. **22:** 517–523.

Hoffman, M., Jia, Z., Pena, M.J., Cash, M., Harper, A., Blackburn II, A.R., Darvill, A., and York, W.S. (2005). Structural analysis of xyloglucans in the primary cell walls of plants in the subclass *Asteridae.* Carbohydr. Res. **340:** 1826–1840.

Hoof, A., and Green, P.J. (1996). Premature nonsense codons decrease the stability of phytohemagglutinin mRNA in a position-dependent manner. Plant J. **10:** 415–424.

Hough, L., Jones, J.V.S., and Wuseman, P. (1972). On the automated analysis of neutral monosaccharides in glycoproteins and polysaccharides. Carbohydr. Res. **21:** 9–17.

Karimi, M., Inze, D., and Depicker, A. (2002). Gateway vectors for *Agrobacterium*-mediated plant transformation. Trends Plant Sci. **7:** 193–195.

Keegstra, K., Talmadge, K.W., Bauer, W.D., and Albersheim, P. (1973). The structure of plant cell walls. III. A model of the walls of suspension-cultured sycamore cells based on the interconnections of the macromolecular components. Plant Physiol. **51:** 188–196.

Kiefer, L.L., York, W.S., Albersheim, P., and Darvill, A.G. (1990). Structural characterization of an arabinose-containing heptadecasaccharide enzymically isolated from sycamore extracellular xyloglucan. Carbohydr. Res. **197:** 139–158.

Kim, C.M., Park, S.H., Je, B.I., Park, S.H., Park, S.J., Piao, H.L., Eun, M.Y., Dolan, L., and Han, C.-d. (2007). *OsCSLD1*, a cellulose synthase-like *D1* gene, is required for root hair morphogenesis in rice. Plant Physiol. **143:** 1220–1230.

Knox, J.P., Linstead, P.J., King, J., Cooper, C., and Roberts, K. (1990). Pectin esterification is spatially regulated both within cell walls and between developing tissues of root apices. Planta **181:** 512–521.

Knox, J.P., Peart, J., and Neill, S.J. (1995). Identification of novel cell surface epitopes using a leaf epidermal-strip assay system. Planta **196:** 266–270.

Lerouxel, O., Cavalier, D.M., Liepman, A.H., and Keegstra, K. (2006). Biosynthesis of plant cell wall polysaccharides - A complex process. Curr. Opin. Plant Biol. **9:** 621–630.

Lerouxel, O., Choo, T.S., Seveno, M., Usadel, B., Faye, L., Lerouge, P., and Pauly, M. (2002). Rapid structural phenotyping of plant

cell wall mutants by enzymatic oligosaccharide fingerprinting. Plant Physiol. **130:** 1754–1763.

Li, X., Cordero, I., Caplan, J., Molhoj, M., and Reiter, W.-D. (2004). Molecular analysis of 10 coding regions from *Arabidopsis* that are homologous to the MUR3 xyloglucan galactosyltransferase. Plant Physiol. **134:** 940–950.

Lorences, E.P., and Fry, S.C. (1994). Sequencing of xyloglucan oligosaccharides by partial Driselase digestion: The preparation and quantitative and qualitative analysis of two new tetrasaccharides. Carbohydr. Res. **263:** 285–293.

Madson, M., Dunand, C., Li, X.L., Vanzin, G.F., Caplan, J., Shoue, D.A., Carpita, N., and Reiter, W.D. (2003). The *mur3* gene of *Arabidopsis* encodes a xyloglucan galactosyltransferase that is evolutionarily related to animal exostosins. Plant Cell **15:** 1662–1670.

Maruyama, K., Goto, C., Numata, M., Suzuki, T., Nakagawa, Y., Hoshino, T., and Uchiyama, T. (1996). *O*-acetylated xyloglucan in extracellular polysaccharides from cell-suspension cultures of *Mentha.* Phytochemistry. **41:** 1309–1314.

McCann, M.C., and Roberts, K. (1991). Architecture of the primary cell wall. In The Cytoskeletal Basis of Plant Growth and Form, C.W. Lloyd, ed (London: Academic Press), pp. 109–129.

McCartney, L., Marcus, S.E., and Knox, J.P. (2005). Monoclonal antibodies to plant cell wall xylans and arabinoxylans. J. Histochem. Cytochem. **53:** 543–546.

Meinke, D., and Koornneef, M. (1997). Community standards for *Arabidopsis* genetics. Plant J. **12:** 247–253.

Muller, M., and Schmidt, W. (2004). Environmentally induced plasticity of root hair development in *Arabidopsis.* Plant Physiol. **134:** 409–419.

Nguema-Ona, E., Andeme-Onzighi, C., Aboughe-Angone, S., Bardor, M., Ishii, T., Lerouge, P., and Driouich, A. (2006). The *reb1-1* mutation of *Arabidopsis.* Effect on the structure and localization of galactose-containing cell wall polysaccharides. Plant Physiol. **140:** 1406–1417.

Obel, N., Erben, V., and Pauly, M. (2006). Functional wall glycomics through oligosaccharide mass profiling. In The Science and Lore of the Plant Cell Wall. Biosynthesis, Structure & Function, T. Hayashi, ed (Boca Raton, FL: Brown Walker Press), pp. 258–266.

Obel, N., Neumetzler, L., and Pauly, M. (2007). Hemicelluloses and cell expansion. In The Expanding Cell, J.-P. Verbelen and K. Vissenberg, eds (Berlin: Springer-Verlag), pp. 57–88.

Obro, J., Harholt, J., Scheller, H.V., and Orfila, C. (2004). Rhamnogalacturonan I in *Solanum tuberosum* tubers contains complex arabinogalactan structures. Phytochemistry. **65:** 1429–1438.

O'Neill, M.A., and York, W.S. (2003). The composition and struture of plant primary cell walls. In The Plant Cell Wall, J.K.C. Rose, ed (Boca Raton, FL: CCRC Press), pp. 1–54.

Passioura, J., and Fry, S. (1992). Turgor and cell expansion: Beyond the Lockhart equation. J. Funct. Plant Biol. **19:** 565–576.

Pauly, M., Albersheim, P., Darvill, A., and York, W.S. (1999a). Molecular domains of the cellulose/xyloglucan network in the cell walls of higher plants. Plant J. **20:** 629–639.

Pauly, M., Andersen, L.N., Kauppinen, S., Kofod, L.V., York, W.S., Albersheim, P., and Darvill, A. (1999b). A xyloglucan-specific endo-β-1,4-glucanase from *Aspergillus aculeatus*: Expression cloning in yeast, purification and characterization of the recombinant enzyme. Glycobiology **9:** 93–100.

Pena, M.J., Ryden, P., Madson, M., Smith, A.C., and Carpita, N.C. (2004). The galactose residues of xyloglucan are essential to maintain mechanical strength of the primary cell walls in *Arabidopsis* during growth. Plant Physiol. **134:** 443–451.

Perrin, R., Jia, Z., Wagner, T.A., O'Neill, M., Sarria, R., York, W.S., Raikhel, N.V., and Keegstra, K. (2003). Analysis of xyloglucan fucosylation in *Arabidopsis.* Plant Physiol. **132:** 678–778.

Perrin, R., Wilkerson, C., and Keegstra, K. (2001). Golgi enzymes that synthesize plant cell wall polysaccharides: Finding and evaluating candidates in the genomic era. Plant Mol. Biol. **47:** 115–130.

Perrin, R.M., DeRocher, A.E., Bar-Peled, M., Zeng, W., Norambuena, L., Orellana, A., Raikhel, N.V., and Keegstra, K. (1999). Xyloglucan fucosyltransferase, an enzyme involved in plant cell wall biosynthesis. Science **284:** 1976–1979.

Popper, Z.A., and Fry, S.C. (2003). Primary cell wall composition of bryophytes and charophytes. Ann. Bot. (Lond.) **91:** 1–12.

Popper, Z.A., and Fry, S.C. (2004). Primary cell wall composition of pteridophytes and spermatophytes. New Phytol. **164:** 165–174.

Popper, Z.A., and Fry, S.C. (2005). Widespread occurrence of a covalent linkage between xyloglucan and acidic polysaccharides in suspension-cultured angiosperm cells. Ann. Bot. (Lond.) **96:** 91–99.

Puhlmann, J., Bucheli, E., Swain, M.J., Dunning, N., Albersheim, P., Darvill, A.G., and Hahn, M.G. (1994). Generation of monoclonal antibodies against plant cell-wall polysaccharides. I. Characterization of a monoclonal antibody to a terminal α-(1,2)-linked fucosyl-containing epitope. Plant Physiol. **104:** 699–710.

Ray, P.M. (1980). Cooperative action of β-glucan synthetase and UDP-xylose xylosyl transferase of Golgi membranes in the synthesis of xyloglucan-like polysaccharide. Biochim. Biophys. Acta **629:** 431–444.

Reiter, W.-D., Chapple, C., and Somerville, C.R. (1997). Mutants of *Arabidopsis thaliana* with altered cell wall polysaccharide composition. Plant J. **12:** 335–345.

Ryden, P., Sugimoto-Shirasu, K., Smith, A.C., Findlay, K., Reiter, W.-D., and McCann, M.C. (2003). Tensile properties of *Arabidopsis* cell walls depend on both a xyloglucan cross-linked microfibrillar network and rhamnogalacturonan II-borate complexes. Plant Physiol. **132:** 1033–1040.

Sarria, R., Wagner, T.A., O'Neill, M.A., Faik, A., Wilkerson, C.G., Keegstra, K., and Raikhel, N.V. (2001). Characterization of a family of *Arabidopsis* genes related to xyloglucan *Fucosyltransferase1.* Plant Physiol. **127:** 1595–1606.

Schiefelbein, J.W., and Somerville, C. (1990). Genetic control of root hair development in *Arabidopsis thaliana.* Plant Cell **2:** 235–243.

Seifert, G.J., Barber, C., Wells, B., Dolan, L., and Roberts, K. (2002). Galactose biosynthesis in *Arabidopsis*: Genetic evidence for substrate channeling from UDP-D-galactose into cell wall polymers. Curr. Biol. **12:** 1840–1845.

Seifert, G.J., Barber, C., Wells, B., and Roberts, K. (2004). Growth regulators and the control of nucleotide sugar flux. Plant Cell **16:** 723–730.

Selvendran, R.R., March, J.F., and Ring, S.G. (1979). Determination of aldoses and uronic acid content of vegetable fiber. Anal. Biochem. **96:** 282–292.

Sessions, A., et al. (2002). A high-throughput *Arabidopsis* reverse genetics system. Plant Cell **14:** 2985–2994.

Somerville, C., Bauer, S., Brininstool, G., Facette, M., Hamann, T., Milne, J., Osborne, E., Paredez, A., Persson, S., Raab, T., Vorwerk, S., and Youngs, H. (2004). Toward a systems approach to understanding plant cell walls. Science **306:** 2206–2211.

Talbott, L.D., and Ray, P.M. (1992). Molecular size and separability features of pea cell wall polysaccharides. Plant Physiol. **98:** 357–368.

Thompson, D.S. (2005). How do cell walls regulate plant growth? J. Exp. Bot. **56:** 2275–2285.

Vanzin, G.F., Madson, M., Carpita, N.C., Raikhel, N.V., Keegstra, K., and Reiter, W.D. (2002). The *mur2* mutant of *Arabidopsis thaliana* lacks fucosylated xyloglucan because of a lesion in fucosyltransferase AtFUT1. Proc. Natl. Acad. Sci. USA **99:** 3340–3345.

Veytsman, B.A., and Cosgrove, D.J. (1998). A model of cell wall expansion based on thermodynamics of polymer networks. Biophys. J. **75:** 2240–2250.

Vincken, J.P., York, W.S., Beldman, G., and Voragen, A.G. (1997). Two general branching patterns of xyloglucan, XXXG and XXGG. Plant Physiol. **114:** 9–13.

Wang, X., Cnops, G., Vanderhaeghen, R., De Block, S., Van Montagu, M., and Van Lijsebettens, M. (2001). *AtCSLD3*, a cellulose synthase-like gene important for root hair growth in *Arabidopsis.* Plant Physiol. **126:** 575–586.

Willats, W.G., Orfila, C., Limberg, G., Buchholt, H.C., van Alebeek, G.J., Voragen, A.G., Marcus, S.E., Christensen, T.M., Mikkelsen, J.D., Murray, B.S., and Knox, J.P. (2001). Modulation of the degree and pattern of methyl-esterification of pectic homogalacturonan in plant cell walls. Implications for pectin methyl esterase action, matrix properties, and cell adhesion. J. Biol. Chem. **276:** 19404–19413.

Willats, W.G.T., Limberg, G., Buchholt, H.C., van Alebeek, G.-J., Benen, J., Christensen, T.M.I.E., Visser, J., Voragen, A., Mikkelsen, J.D., and Knox, J.P. (2000). Analysis of pectic epitopes recognised by hybridoma and phage display monoclonal antibodies using defined oligosaccharides, polysaccharides, and enzymatic degradation. Carbohydr. Res. **327:** 309–320.

Yates, E.A., Valdor, J.-F., Haslam, S.M., Morris, H.R., Dell, A., Mackie, W., and Knox, J.P. (1996). Characterization of carbohydrate structural features recognized by anti-arabinogalactan-protein monoclonal antibodies. Glycobiology **6:** 131–139.

York, W., Darvill, A., McNeil, M., Stevenson, T.T., and Albersheim, P. (1985). Isolation and characterization of plant cell walls and cell wall components. In Methods in Enzymology, A. Weissbach and H. Weissbach, eds (Orlando, FL: Academic Press), pp. 3–40.

York, W.S., Kolli, V.S.K., Orlando, R., Albersheim, P., and Darvill, A.G. (1996). The structures of arabinoxyloglucans produced by solanaceous plants. Carbohydr. Res. **285:** 99–128.

York, W.S., Oates, J.E., van Halbeek, H., Darvill, A.G., Albersheim, P., Tiller, P.R., and Dell, A. (1988). Location of the *O*-acetyl substituents on a nonasaccharide repeating unit of sycamore extracellular xyloglucan. Carbohydr. Res. **173:** 113–132.

Zabotina, O., van de Ven, M., Freshour, G., Drakakaki, G., Cavalier, D.M., Mouille, G., Hahn, M.G., Keegstra, K., and Raikhel, N.V. (2008). The *Arabidopsis* XXT5 protein encodes a putative α-1,6-xylosyltransferase that is involved in xyloglucan biosynthesis. Plant J., in press.

This information is current as of March 28, 2012

Supplemental Data	http://www.plantcell.org/content/suppl/2008/05/27/tpc.108.059873.DC1.html
References	This article cites 90 articles, 48 of which can be accessed free at: http://www.plantcell.org/content/20/6/1519.full.html#ref-list-1
Permissions	https://www.copyright.com/ccc/openurl.do?sid=pd_hw1532298X&issn=1532298X&WT.mc_id=pd_hw1532298X
eTOCs	Sign up for eTOCs at: http://www.plantcell.org/cgi/alerts/ctmain
CiteTrack Alerts	Sign up for CiteTrack Alerts at: http://www.plantcell.org/cgi/alerts/ctmain
Subscription Information	Subscription Information for *The Plant Cell* and *Plant Physiology* is available at: http://www.aspb.org/publications/subscriptions.cfm